

NEW YORK UNIVERSITY
COURANT INSTITUTE — LIBRARY
4 Washington Place, New York 3, N. Y.

EM-39

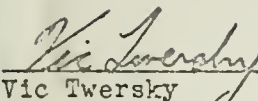
6.1


New York University
Washington Square College of Arts and Science
Mathematics Research Group

Research Report No. EM-39
Contract No. AF-19(122)-42

NEW YORK UNIVERSITY
COCHRAN INSTITUTE - LIBRARY
1 Washington Place, New York 3, N. Y.

MULTIPLE SCATTERING OF RADIATION, PART II
(THE GRATING)
by
VIC TWERSKY


Vic Twersky


Morris Kline
Project Director

The research reported in this document has been made possible through support and sponsorship extended by the Geophysics Research Division of the Air Force Cambridge Research Center, under Contract No. AF-19(122)-42. It is published for technical information only, and does not necessarily represent recommendations or conclusions of the sponsoring agency.

1951?

Table of Contents

	page
Note	ii
Abstract	iii
4.1 Introduction	1
4.2 The Finite Grating of Parallel Cylinders	2
4.21 Complete Solution	2
4.22 Far Field Solution	5
4.23 Spacing Larger than Wavelength	7
4.24 End Effects Neglected, Explicit Solution	12
4.3 Mode Approximations	15'
4.31 " A_0 mode": Isotropic Scatterers	16
4.311 Qualitative Analysis of the Solution	18
4.312 Numerical Analysis of the Solution	27
4.32 " A_1 mode"	34
4.33 " $A_0 + A_1$ mode"	35
4.4 The Reflection Grating of Bosses on a Plane	37
4.5 Extension of the Theory to Gratings with Elements other than Cylinders	48
Appendix - Wilhelm Magnus	

Note

This report is section 4 of a series of papers on multiple scattering of radiation. The first three sections, dealing respectively with an arbitrary configuration of parallel cylinders, a planar configuration, and two cylinders will be found in Research Report EM-34. Formal solutions satisfying any of the usually prescribed boundary conditions at the surface of each cylinder were obtained for the previous scattering problems by explicitly taking into account all contributions to the excitation of each cylinder by the radiation the remaining cylinders scattered. The solution was expressed as the incident wave plus a sum of an infinite number of "orders of scattering". The first order, the usual single scattering approximation, resulted from the excitation of each cylinder by only the incident plane wave; the second order arose from the excitation of each element by the first order of scattering from the remaining elements, etc. In the present report we will consider the multiple scattering of radiation by a finite grating of parallel cylinders. To obviate repetition the results of the previous report will be referred to wherever feasible.

4. THE GRATING

4.1. Introduction

The problem of a plane wave normally incident on a finite grating of parallel circular cylinders of infinite length was treated by Schaefer and Reiche¹ subject to the single scattering hypothesis, i.e., by neglecting all excitations of each cylinder due to the waves the remaining cylinders scatter. They showed that if the width of the grating was small compared to the distance of observation, the singly scattered wave could be approximated by

$$(4.1) \quad \psi^1 = \psi^0 \sin(N\gamma) / \sin \gamma, \quad \gamma = Kb \sin \theta,$$

where N is the number of elements, b is the spacing, r and θ are measured from the axis of the central cylinder, and the superscript 1 merely indicates that this corresponds to our first order of scattering. The function ψ^0 is the scalar of the appropriate Hertz vector potential of the wave the central cylinder scatters when excited only by the plane wave.

The problem was then reformulated by the writer² who considered the excitation of each cylinder as the incident plane wave plus the waves scattered by its nearest neighbors as a result of plane wave excitation. A crude criterion for the range of validity of the single scattering hypothesis was obtained by showing that all terms arising from these additional excitations approached zero more rapidly with decreasing radius or increasing spacing than did those of (4.1). In this paper we will treat the finite grating of cylinders (and of semicylindrical bosses on an infinite plane) by specializing the formal solution obtained previously for an arbitrary configuration of parallel cylinders³. All multiple excitations of each cylinder arising from the waves scattered by the remaining cylinders will be taken into account explicitly.

In Section 4.21 the complete solution will be written down and the various orders of scattering interpreted. In Section 4.22 the far field for distance of observation large compared to the width of the grating, for which restrictions the first order of scattering reduces essentially to the solution of Schaefer and Reiche, will be obtained. The restriction that the spacing is large compared to $\lambda/2\pi$ is introduced in Section 4.23, and the wavelengths for which the multiply scattered orders are either maxima or minima are determined. In Section 4.24 the end effects of the finite grating are neglected and the multiply scattered orders

-
1. C.Schaefer and F.Reiche, Ann. Physik 35, 817(1911). The writer is grateful to Prof. Reiche for suggesting this problem and to Prof.J.B.Keller and Dr.J.Shmoys for many fruitful discussions.A representative bibliography of the infinite grating, which can be formulated exactly by means of an integral equation, as well as, a variational approach to the problem, will be found in J.Shmoys, J.Opt. Soc.Am. 41, 324 (1951).
 2. V. Twersky, J. Acoust. Soc. Am. 22, 539 (1950).
 3. V. Twersky, "Multiple Scattering of Radiation, Part I", EM-34, Math.Res.Grp., NYU; WSC, 1951.

summed explicitly. Approximate solutions for radii very small compared to wavelength are obtained in Section 4.3 and investigated in detail. Because of the presence of hitherto untabulated functions in these expressions, they are first analyzed qualitatively and the forms of the intensity curves deduced before the results of numerical computations are presented. In Section 4.4 the analogous grating of semicylindrical bosses on an infinite plane is considered, and in Section 4.5 the extension of the present theory to gratings with elements other than cylinders is discussed.

Employing the approximate solutions of Section 4.3 we obtain an analytic criterion for the range of validity of the single scattering approximation and the wavelengths for which the effects of multiple scattering are maximal, or give rise to the greatest departures from the predictions of single scattering theory. It is of interest to note that the predicted maximal effects are quite similar to the "grating anomalies" or "Wood anomalies" observed by Wood⁴, Strong⁵, and Ingersoll⁶ in the white light spectra of certain reflection gratings. The present analysis provides a simple and physically plausible interpretation for the occurrence of the pronounced bright and dark bands observed for certain wavelengths based on the magnitudes and phases of the various orders of scattering, and also correlates more of the observed phenomena than does Rayleigh's "dynamical theory of the grating"⁷.

4.2 The Finite Grating of Parallel Cylinders

4.21 Complete Solution

In this section we will specialize the results obtained previously in Section 2, reference 3, for an arbitrary planar configuration of parallel cylinders to obtain a multiple scattering solution for the finite grating of identical cylinders. As in Fig. 4.2, we consider a plane wave $\psi_1 = \exp[iKr \cos(\theta + \alpha)]$, the velocity potential for acoustics or the scalars of the Hertz vector potentials for electromagnetics as in Section 1.5, incident on a grating of $N = 2N+1$ cylinders of radii a and spacing b . For symmetry purposes the reference origin of coordinates r, θ , is taken on the axis of the central cylinder at the intersection of its axis with the xy -plane.

4. R.W. Wood, Phil. Mag. 36 (1902); 23, 310 (1912); Phys.Rev. 48, 928 (1935).

5. J. Strong, Phys. Rev. 49, 291 (1936).

6. L.R. Ingersoll, Astrophysical Journal 51, 129 (1920); Phys.Rev. 17, 493 (1921).

7. Rayleigh, Proc.Roy.Soc.London A79, 399 (1907); see also U.Fano, Phys.Rev. 50 573 (1936); 51, 288 (1937). Rayleigh had also deduced the occurrence of anomalies for certain wavelengths in an earlier paper, Phil.Mag. 14, 60 (1907), by arguments based on potential theory and inspection of the spectrograms obtained by Wood in his 1902 paper.

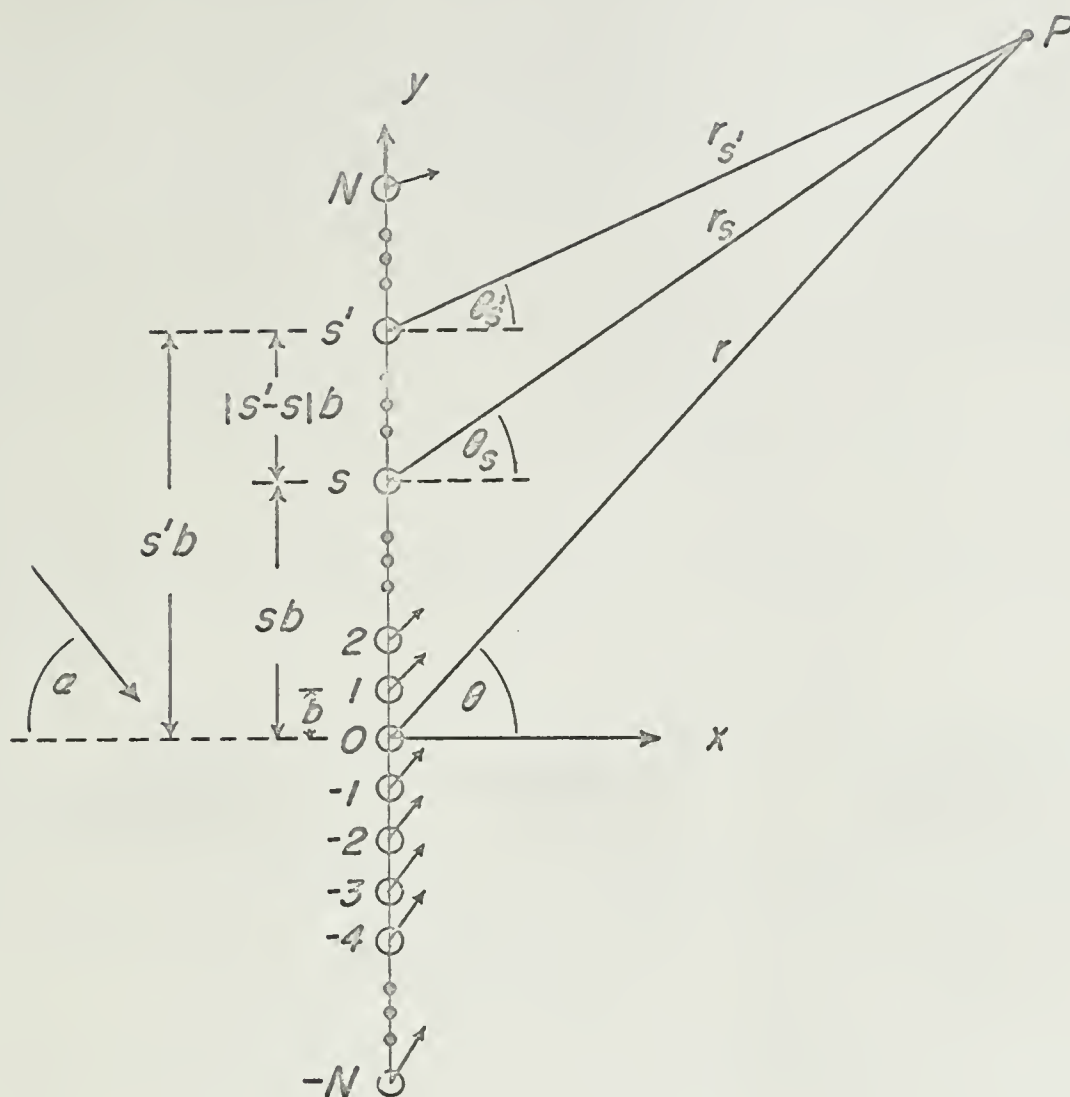


Fig. 4.1

The wave scattered by a planar configuration of identical cylinders as in (2.5) can be written as

$$(4.2) \psi = \sum_{n=-\infty}^{\infty} A_n i^n \sum_s H_n(Kr_s) \exp(in\theta_s - iKy_s \sin\alpha) \sum_{m=1}^{\infty} \left\{ \prod_{\mu=1}^{(m-1)} \sum_{n^{\mu}} A_{n^{\mu}} i^{-n^{\mu}-1} + n^{\mu} \sum_{s^{\mu}}' H_{n^{\mu}-1-n^{\mu}}(Ky_{s^{\mu}-1} s^{\mu}) \right. \\ \left. \times \exp[-ic_{s^{\mu}-1} s^{\mu} (Ky_{s^{\mu}-1} s^{\mu} \sin\alpha + [n^{\mu-1} - n^{\mu}] \pi/2)] \right\} \exp[in(m-1)\alpha],$$

where A_n are the scattering coefficients of the single cylinder (e.g., $A_n = -J_n(Ka)/H_n(Ka)$ for $\psi + \psi_i$ to vanish at each cylinder, etc.), the H 's are the Hankel functions of the first kind to correspond to outgoing waves for the suppressed time factor $\exp(-i\omega t)$, r_s and θ_s locate an observation point P in the coordinate frame of the s -th cylinder (the polar axis, x , being perpendicular to the plane of the configur-

ation), y_s is the distance of the s -th cylinder from the reference origin, $y_{ss'}$ is the separation of any two cylinders, \sum' indicates that $s^\mu = s^{\mu-1}$ is to be excluded from the sum, and $\epsilon_{s^\mu, s^{\mu-1}} = \pm 1$ for $s^\mu \geq s^{\mu-1}$. For $m=1$, the first order of scattering, the formal product over μ (μ indicating the number of primes distinguishing the indices) reduces to unity, and the sum over m (m indicating the orders of scattering) reduces to $\exp(in\alpha)$. On substituting $y_s = sb$, $y_{ss'} = |(s'-s)b| = \epsilon_{ss'}(s'-s)b$, etc., and suppressing K and Kb and letting $bsin\alpha = A$ for brevity, we obtain

$$(4.3) \quad \psi = \sum_n A_n i^n \sum_{s=-N}^N H_n(r_s) \exp(in\theta_s - isA) \sum_m \left\{ \prod_{n^\mu} A_{n^\mu} S_{n^{\mu-1}, n^\mu} \right\} \exp[in^{(m-1)}\alpha] ,$$

$$S_{n^{\mu-1}, n^\mu} = i^{-n^{\mu-1} + n^\mu} \sum_{s^\mu}' H_{n^{\mu-1} - n^\mu}(|s^\mu - s^{\mu-1}|) \exp \left\{ -i\epsilon_{s^\mu, s^{\mu-1}} \left[|s^\mu - s^{\mu-1}| A + (n^{\mu-1} - n^\mu) \pi/2 \right] \right\}.$$

This expression when added to ψ_1 constitutes a formal solution for the problem of the grating satisfying prescribed boundary conditions simultaneously at each cylinder.

We split the sums over s^μ into two partial sums corresponding to s^μ greater and s^μ less than $s^{\mu-1}$ and introduce the positive separation index $\sigma^{\mu-1} = |s^\mu - s^{\mu-1}|$ to obtain

$$(4.4) \quad S_{n^{\mu-1}, n^\mu} = (-1)^{n^{\mu-1} + n^\mu} \sum_{\sigma^{\mu-1}=1}^{N-s^{\mu-1}} H_{n^{\mu-1} - n^\mu}(\sigma^{\mu-1}) \exp(-i\sigma^{\mu-1}A) + \sum_{\sigma^{\mu-1}=1}^{N+s^{\mu-1}} H_{n^{\mu-1} - n^\mu}(\sigma^{\mu-1}) \exp(i\sigma^{\mu-1}A)$$

$$= \sum \epsilon_- (\sigma^{\mu-1}) + \sum \epsilon_+ (\sigma^{\mu-1}),$$

where it is understood that $s^{\mu-1} \neq N$ in the first sum, and $s^{\mu-1} \neq -N$ in the second. The quantity $S_{n^{\mu-1}, n^\mu}$, the "multiple excitation factor", consists essentially of two finite Schlomilch series⁸ (i.e., of the form $\sum_p \frac{a_p}{p} Z_q(pX)$), for which unfortunately no explicit representations exist. The present problem is therefore much more complicated than that of two cylinders, Section 3, where we dealt merely with the first term of a series of this type.

To facilitate discussion of their physical significance, the various orders of scattering can be expressed as

$$(4.5) \quad \psi^1 = \sum A_n \exp(in\alpha) \Delta_1, \quad \psi^2 = \sum A_n \sum A_{n'} \exp(in'\alpha) \Delta_2,$$

$$\psi^3 = \sum A_n \sum A_{n'} \sum A_{n''} \exp(in''\alpha) \Delta_3, \text{ etc.,}$$

where

$$(4.6) \quad \Delta_1 = \sum_{s=-N}^N f(s) \quad , \quad f(s) = i^n H_n(r_s) \exp(in\theta_s - isA) \quad ,$$

$$\Delta_2 = \Delta_1 S_{nn'} = \sum_{s=-N}^{N-1} \sum_{\sigma=1}^{N-s} \left\{ f(s) g_{-}(\sigma) + f(-s) g_{+}(\sigma) \right\} \quad ,$$

$$\begin{aligned} \Delta_3 = \Delta_2 S_{nn''} = & \sum_{s=-N}^{N-2} \sum_{\sigma=1}^{N-s-1} \sum_{\sigma'=1}^{N-s-\sigma} \left\{ f(s) g_{-}(\sigma) g_{-}(\sigma') + f(-s) g_{+}(\sigma) g_{+}(\sigma') \right\} \\ & + \sum_{s=-N}^{N-1} \sum_{\sigma=1}^{N-s} \sum_{\sigma'=1}^{N+s+\sigma} \left\{ f(s) g_{-}(\sigma) g_{+}(\sigma') + f(-s) g_{+}(\sigma) g_{-}(\sigma') \right\} \quad , \text{ etc.} , \end{aligned}$$

$f(-s)$ being $f(s)$ with s replaced by $-s$, and the various g 's as defined in (4.4)

The quantities Δ_m characterize each order of scattering. Thus the first order comprises $2N+1$ terms corresponding to the waves singly scattered by each cylinder; the second order comprises $2N(2N+1)$ terms, each of the $2N+1$ cylinders scattering $2N$ waves as a result of its excitation by the waves scattered by the remaining $2N$ elements; and similarly the m -th order comprises $(2N)^{m-1}(2N+1)$ terms. The differences in the upper limits of the corresponding sums of the various orders of scattering is a consequence of the finite number of elements in the grating, i.e., of the "end effects" of the finite grating. Thus the exclusion of $s=N$ from Δ_2 merely indicates that there are no cylinders above the N -th, or below the $-N$ -th, to contribute to the excitation of these cylinders. Similarly the exclusion of $s=N, N-1$, from the "diagonal terms" of Δ_3 indicate, for example, that cylinder $s=N-2$ is the highest cylinder whose tertiary excitations arise from the second order of scattering of a cylinder lying above it which in turn possesses a secondary excitation from a still higher cylinder, etc. It can be seen that the highest order of scattering possessing diagonal terms (i.e., containing only g_{-} or g_{+}) is $m = \mathcal{N}$.

There is little that can be done with the solution in its present form. The usual first order of scattering is itself not amenable to numerical calculations without the introduction of suitable approximations, and the complexity of the higher orders increases as the power of m . For an infinite grating the limits of the sums in (4.6) would be replaced by $s = -\infty$ to $+\infty$ and $\sigma = 1$ to ∞ , thereby eliminating the bookkeeping that the finite grating requires. Furthermore were it possible to eliminate the dependence of the g 's on the indices n^μ , the various Δ 's would reduce to actual products of the form $\Delta_m = \Delta_1 S^{m-1}$ and the total scattered wave to a simple geometric progression that could be summed explicitly. Our goal is to obtain approximate solution of this form by imposing suitable restrictions on the parameters of the problem.

4.22 Far Field Solution

We will now obtain the far field solution for distance of observation

large compared to the width of the grating. For $Kr \gg 1$, $Kr \gg |n|$ (the second condition restricting the parameters of the cylinder so that the A_n decrease rapidly with increasing n), we can employ $H_n(r_s) \rightarrow (2/i\pi Kr_s)^{1/2} i^{-n} \exp(iKr_s) = H_0(r_s) i^{-n}$, where it is understood that H_0 is the asymptotic form. In addition, for $r \gg \lambda b$ we have $r_s \approx r - sb \sin \theta \approx r - sT$ and $\theta_s \approx \theta - (sb/r_s) \cos \theta \rightarrow \theta$, so that $H_0(r_s) \rightarrow H_0(r) \exp(-isT)$ on neglecting $sT \ll r_s$ in the denominator of the square root in $H_0(r_s)$. Hence (4.3) reduces to

$$(4.7) \quad \psi = H_0(r) \sum_n A_n e^{in\theta} \sum_s e^{-is\gamma} \sum_m \left\{ \prod_{\mu} \sum_{n^{\mu}} A_{n^{\mu}} S_{n^{\mu}-n} \right\} \exp[in(m-1)\alpha],$$

where $\gamma = T+A = Kb(\sin \theta + \sin \alpha)$.

Factoring $H_0(r) \exp(in\theta)$ from the quantities of (4.6), but retaining the symbol Δ for simplicity, yields

$$(4.8) \quad \Delta_1 = \sum_{s=-N}^N e^{-is\gamma} = \sin(\lambda\gamma/2) / \sin(\gamma/2) \equiv \Delta(\lambda),$$

$$\Delta_2 = \sum_{s=-N}^{N-1} \sum_{\sigma=1}^{N-s} H_{n-n'}(\sigma) \left\{ (-1)^{n+n'} e^{-i(s\gamma+\sigma A)} + e^{i(s\gamma+\sigma A)} \right\}$$

$$= \sum_{\sigma=1}^{\lambda-1} H_{n-n'}(\sigma) \Delta(\lambda-\sigma) \left\{ (-1)^{n+n'} e^{i\sigma\gamma'/2} + e^{-i\sigma\gamma'/2} \right\},$$

$$\Delta_3 = \left\{ \sum \sum \sum \left[(-1)^{n+n''} e^{-i[s\gamma+(\sigma+\sigma')A]} + e^{i[s\gamma+(\sigma+\sigma')A]} \right] \right.$$

$$\left. + \sum \sum \sum \left[(-1)^{n+n'} e^{-i[s\gamma+(\sigma-\sigma')A]} + (-1)^{n'+n''} e^{i[s\gamma+(\sigma-\sigma')A]} \right] \right\} H_{n-n'}(\sigma) H_{n'-n''}(\sigma'), \text{etc.}$$

The quantity $\Delta_1 = \Delta(\lambda)$, a geometric progression which we have summed explicitly, is the usual Fraunhofer "grating factor", and ψ^1 is essentially that obtained by Schaefer and Reiche¹. For the second order, Δ_2 , we have interchanged the order of summation and summed over s to facilitate future calculations, $\Delta(\lambda-\sigma)$ being $\Delta(\lambda)$ with λ replaced by $\lambda-\sigma$, and γ' equalling $T-A$. The limits of the sums in Δ_3 for the third order are as in (4.6).

Before introducing additional restrictions to simplify the solution a few remarks on the behavior of the first order of scattering, or of a Fraunhofer grating⁹, are in order. The principal maxima of the first order of scattering (neglecting the "envelope" corresponding to the single cylinder solution which in the present problem takes the place of the usual "single slit factor") occur when

9. See for example F.A. Jenkins and H.E. White, Physical Optics, Ch. 7, McGraw Hill, N.Y., 1937.

$$(4.9) \quad \gamma = Kb(\sin\theta + \sin\alpha) = 2q\pi, \quad q = 0, \pm 1, \pm 2 \dots,$$

for which values $\Delta(\mathcal{N})$ reduces to \mathcal{N} , the number of elements. The q 's are the spectral orders or spectra of the grating, the + sign corresponding to those found in a counter-clockwise direction from the incident wave normal, and the - sign to those clockwise. The minima of $\Delta(\mathcal{N})$, equalling zero, occur when $\mathcal{N}\gamma = 2q\pi$, $\gamma \neq 2q\pi$, so that there are $\mathcal{N}-1$ minima and $\mathcal{N}-2$ small secondary maxima between two principal maxima. We have employed the notion of a " Δ -function in \mathcal{N} " to indicate the above behavior, and will concern ourselves only with the principal maxima in following discussions. The maxima of the scattered intensity for a grating governed by $\Delta(\mathcal{N})$ occur for wavelengths and angles of observation satisfying $\lambda = b(\sin\theta + \sin\alpha)/q$, or when the path difference of the primary excitation at adjacent cylinders plus their path difference to the observation point equal an integral number of wavelengths. Thus when white light or other broadband radiation is incident on such a grating, the central maximum at $\theta = -\alpha$ (or at $\theta = \pi + \alpha$) will appear white, while on each side will appear the various orders of continuous spectra. We accept the relation $\gamma = 2q\pi$ as a labeling device enabling us to associate a particular wavelength with a set of angles of observation (or an interrelated sequence of wavelengths with a particular angle). We will consider the factors in γ appearing in all orders of scattering as yielding the angular distribution of the total scattered radiation, the remaining factors being essentially but source strengths whose values can modify the amplitude of a particular angular component but not alter its position.

4.23 Spacing Larger than Wavelength

It is evident from (4.9) that for a planar configuration of equally spaced parallel elements to function physically as a grating we require that the spacing be at least as large as the wavelength for even one spectral order to be observed, twice as large for two, etc. Hence the restriction that the spacing be large compared to $\lambda/2\pi$ that we now introduce explicitly is perforce tacit in all treatments of the grating. For $Kb \gg 1$, $Kb \gg |n^{\mu-1} - n^{\mu}|$ we will employ $H_{n^{\mu-1} - n^{\mu}}(\sigma^{\mu-1}) \rightarrow H(\sigma) i^{-n^{\mu-1} + n^{\mu}}$, where $H(\sigma) = (2/i\pi Kb\sigma)^{1/2} \exp(i\sigma Kb) \equiv h(\sigma) \exp(i\sigma Kb)$ is the asymptotic form of $H_0(\sigma Kb)$. On substituting into (4.7) and summing the terms for positive and negative values of n^{μ} we obtain

$$(4.10) \quad \psi = H_0 \sum_{\sigma} e^{-i\sigma\gamma} \left[C + \sum_{n, n', n'', \dots} C' S_{nn'} \sum_{m=2}^{\infty} \left\{ \prod_{\mu} C_{n^{\mu}}^0 S_{n^{\mu} n^{\mu+1}} \right\} C''_{n^{(m-1)}} \right]$$

$$S_{n^{\mu} n^{\mu+1}} = \sum_{\sigma^{\mu}=1}^{N-S^{\mu-1}} h(\sigma^{\mu}) \exp[i\sigma^{\mu}(1-A)] + (-1)^{n^{\mu} + n^{\mu+1}} \sum_{\sigma^{\mu}=1}^{N+S^{\mu-1}} h(\sigma^{\mu}) \exp[i\sigma^{\mu}(1+A)],$$

where $C = \sum_{n=0}^{n^*} \epsilon_n A_n \cos n(\theta + \alpha)$ with $\epsilon_n = 1$ for $n=0$, $\epsilon_n = 2$ for $n > 0$,

$C_n^I = \epsilon_n A_n \cos n(\theta + \pi/2)$, $C_n^{II} = \epsilon_n A_n \cos n(\alpha - \pi/2)$, $C_n^0 = \epsilon_n A_n$, and where for $m=2$

the formal product over μ equals unity. The restriction $Kb \gg |n-n'|$ limits the possible values of $(n-n')$ or $2n$, and this in turn restricts the permissible values of Ka , $Ka(k_e - 1)^{1/2}$, etc. appearing in the A_n . The convergence properties of the A_n (see section 1.5) are such that for $Ka \ll 1$ we need consider only $n=0, 1$, while for larger Ka we need consider only terms up to n^* where n^* is of the order of magnitude of $Ka+2$, e.g., for $a \approx \lambda$, retaining only the terms to $n^* = 10$ yields a remainder of the order of only 5% in C . Thus for $Kb \approx 20$ we are restricted more or less to $a \lesssim \lambda/2$, and similarly for other values of Kb . The second restriction on Kb is therefore essentially that $Kb \gg Ka$.

It can be seen that to this order of approximation in Kb the multiply scattered orders are all symmetrical with respect to the grating so that for the analogous grating of semicylindrical bosses on a perfectly conducting plane departures from single scattering theory will occur only for the component polarized perpendicular to the elements. The reader is referred to Section 2 for a discussion of this for an arbitrary planar configuration and also for a discussion of the discrepancies in powers of Kb retained that (4.9) entails. The physical significance of these discrepancies is that from this point on we are neglecting the shielding effects which are most pronounced for closely spaced large cylinders. We minimize these discrepancies by restricting the parameters so that the spacing is large compared to wavelength and to radius.

The various orders of scattering are

$$(4.11) \quad \psi^1 = H_0 \Delta(\alpha) C$$

$$\begin{aligned} \psi^2 &= H_0 \sum_{n,n'} C_n^I C_{n'}^I \sum \sum \left\{ e^{-i(s\gamma + \sigma A)} + (-1)^{n+n'} e^{i(s\gamma + \sigma A)} \right\} e^{i\sigma h(\alpha)} \\ &= H_0 \sum_{n,n'} C_n^I C_{n'}^{II} \sum \Delta(\alpha - \sigma) \left\{ e^{i\sigma\gamma'/2} + (-1)^{n+n'} e^{-i\sigma\gamma'/2} \right\} e^{i\sigma h(\sigma)}, \text{ etc.} \end{aligned}$$

These expressions can be employed for calculations to any order of scattering and to determine the ratio $|\psi^2/\psi^1|$, the smallness of which will serve as a criterion for the range of validity of the single scattering approximation. It can be seen that for the second order, containing $S_{nn'}$, the multiple excitation of the s -th cylinder possess phase factors of the form $\exp[i\sigma(1 \pm A)] = \exp[i\sigma Kb(1 \pm \sin \alpha)]$; the term in σKb corresponds to the path difference between the s -th cylinder and the sources of its excitation s' , while the term in $\pm \sigma Kb \sin \alpha$ is the phase

lead or lag of the initial or plane wave excitation at s' relative to that at s . Similarly for the third order, possessing $S_{nn'} S_{n'n''}$, the phase factors are of the form $\exp[i\sigma(1\pm A) \pm i\sigma'(1\pm A)]$, where any combination of signs is permissible.

In spite of the complexity of (4.10) certain interesting conclusions about the wavelengths yielding the "maximal effects" of multiple scattering, or the greatest departures from the predictions of single scattering theory, can be reached immediately. (For that matter these conclusions follow from rather elementary physical considerations for a grating with arbitrary identical elements.) It can be seen from (4.10) that when

$$(4.12) \quad Kb(1 \pm \sin \alpha) = 2p_{\pm} \pi, \quad p_{\pm} = 1, 2, 3 \dots$$

or when $Kbs \sin \alpha = 2p' \pi$, $Kb = 2p \pi$ where p' and p are both integral (corresponding to p_+ and p_- having even parity), or both half odd integral (p_+ and p_- having odd parity), the phase factors of the S 's reduce to unity. The physical significance of integral p' , is that the primary excitation for these wavelengths is in phase at all cylinders (essentially as for normal incidence), while p integral means that the wavelengths are integral fractions of the spacing; these two conditions insure that the multiple excitations of each cylinder due to the remaining cylinders are in phase in any particular order of scattering. Similarly for p' and p both half odd integral, although the primary excitation of neighboring cylinders is 180° out of phase, the fact that the spacing is an odd half integral number of wavelengths insures that the excitations of each element in each order are in phase. Hence the total excitation of all cylinders, or of the grating, are in phase in any particular order and the additional condition (4.9) insures that the waves scattered by all cylinders in each order are in phase at P . Thus each order of scattering is a maximum for angles of incidence, wavelengths, and angles of observation specified by

$$(4.13) \quad \sin \alpha = \frac{p_+ - p_-}{p_+ + p_-}, \quad \lambda = \frac{2b \sin \alpha}{p_+ - p_-} = \frac{2b}{p_+ + p_-}, \quad \sin \theta = \frac{2q - p_+ + p_-}{p_+ + p_-}.$$

Now since the magnitude of each order of scattering must be large for any effects of multiple scattering to be appreciable, we conclude that the most pronounced, or maximal, effects occur in the vicinities of these values.

Whether the intensity is increased or decreased relative to its single scattered value for the vicinity of these wavelengths depends on the phase relations among the various orders of scattering. Thus if all orders are in phase they reinforce the first and the intensity is increased, while if successive orders are 180° out of phase they partially annul the first and the intensity is less than its single scattered value. The present complexity of our expressions precludes

determination of the actual maximal wavelengths for which each order of scattering has its largest value subject to the requirements that successive orders are either in or out of phase. Successive orders differ in phase not only because of the path differences involved (and which are eliminated by (4.12,9)) but also because of the presence of the scattering coefficients of the single cylinder which are complex quantities, and because of the multiples of $-\pi/4$ arising from the waves being cylindrical; nor is it even clear that each order differs from its preceding order by a common phase. In a future section, after we have obtained relatively simple approximate solutions, we will determine the maximal wavelengths for various boundary conditions.

In a similar fashion we can deduce the conditions for the minimal effects of multiple scattering, or the wavelengths for which single scattering theory is most valid. Thus when

$$(4.14) \quad K b(1 \pm \sin \alpha) = p_{\pm}^0 \pi, \quad p_{\pm}^0 = 1, 3, 5 \dots,$$

the total excitation of each element is a minimum, the initial phase difference at neighboring elements plus the phase difference due to the spacing introducing a total phase difference of 180° between the excitations of each element arriving from successive neighbors. Hence half of the excitations of each element in each order are out of phase with the remaining half so that the wave it scatters in each order is minimized, and similarly for the remaining elements. Since this obtains for all orders, regardless of the phases of the orders, we expect the least effects of multiple scattering for the values specified by (4.14).

In addition to the maximal effects occurring in the vicinity of the wavelengths of (4.12) we also expect that fairly large effects will occur in the vicinity of wavelengths satisfying only one of these conditions, i.e., either

$$(4.12') \quad K_+ b(1 + \sin \alpha) = 2p_+ \pi \quad \text{or} \quad K_- b(1 - \sin \alpha) = 2p_- \pi,$$

for which a certain amount of reinforcement among the multiple excitations of each element occurs, e.g., the first insures that waves from successive elements traveling "up" the grating, or in the positive y-direction, are in phase for the second order of scattering, etc.

These conditions were first proposed by Rayleigh⁷ after examining spectrograms obtained by Wood⁴ which showed marked departures from the predictions of Fraunhofer theory; Rayleigh later derived these conditions analytically in his dynamical theory of the grating. His interpretation of their physical significance was as follows: since the wavelengths of (4.12') have principal maxima in the plane of the grating, the excitations of the elements are greatest for these wavelengths. It is therefore expected as a consequence that these wavelengths will appear most intense in the spectral orders of the grating. This sort of interpretation, however, does not suffice for the intensity minima observed for certain wavelengths, nor for the phenomena

of wavelengths possessing maxima in certain spectral orders and minima in others. The multiple scattering interpretation suffices, when the remaining phase factors are taken into account explicitly.

It should be noted that a physical interpretation analogous to that employed by Rayleigh for the maximal wavelengths may also be employed for the minimal wavelengths of (4.14). The Fraunhofer factor, $\Delta(\mathcal{N})$ reduces to -1 in the plane of the grating for the wavelengths of (4.14). The excitations of the higher orders of scattering are therefore quite weak for these wavelengths so that departures from Fraunhofer theory should be negligible.

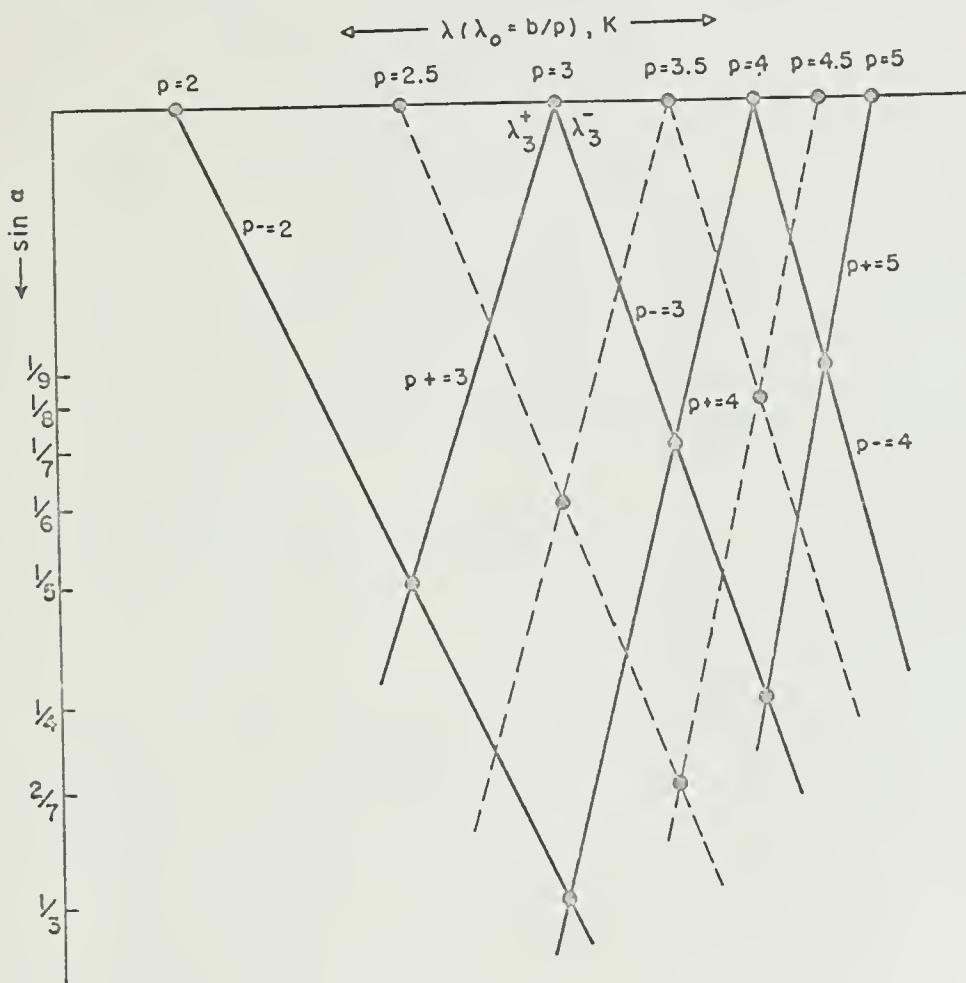


Fig. 4.2

For future convenience we have plotted in Fig. 4.2 the values of K and $\sin \alpha$ corresponding to the individual conditions of the sets (4.12) and (4.14).

The heavy lines correspond to the former, and the dotted lines to the latter, while the circled intersections indicate fulfillment of both conditions of either set. It will be shown later that the actual maximal and minimal wavelengths are displaced only slightly from these positions for the cases to be considered. (It should be noted that Fig. 4.2 is essentially a schematic of the series of correlated spectrograms obtained by Wood (reference 4, 1935) with reversed λ -axis.)

For the wavelengths and angles of (4.9) and (4.12) the S's of (4.10) reduce to

$$(4.15) \quad S_{n^{\mu-1}n^{\mu}} = \sum_{\sigma=1}^{N-s^{\mu-1}} h(\sigma^{\mu}) + (-1)^{n^{\mu-1}-n^{\mu}} \sum_{\sigma=1}^{N+s^{\mu-1}} h(\sigma^{\mu}),$$

while the various orders equal

$$(4.15') \quad \psi^1 = H_0 \mathcal{N} C, \quad \psi^2 = 2H_0 C_e^1 C_e^2 (2/i\pi K b)^{1/2} \sum_s \sum_{\sigma} \sigma^{-1/2},$$

$$\psi^3 = 2H_0 C_e^1 \sum_{n', n''} C_n^0, C_{n_e}^{II} (2/i\pi K b) \left[\sum \sum \sum + (-1)^{n'+n''} \sum \sum \sum \right] (\sigma \sigma')^{-1/2}, \text{ etc.}$$

where C_e^1 and C_e^2 are the sums of the even terms of C_n^1 and C_n^2 , and where $C_{n_e}^{II}$ indicates that only the even terms of C_n^{II} are involved. Although the expressions have simplified considerably for these values, the interdependence of the limits of the sums arising from the end effects preclude explicit summation of the multiply scattered orders. To further the analysis we will employ the artifice of neglecting the end effects in the following sections.

4.24 End Effects Neglected. Explicit Solution

For a grating consisting of an infinite number of elements, the excitation of each cylinder has the same form in any order of scattering regardless of its position in the grating (the excitation of all cylinders being identical for normal incidence), since each element has just as many elements below it contributing to its excitation as it has above. The limits of the sums over s would then be infinite and the sums over σ would go from 1 to ∞ , and would be independent of the indices of the preceding sums, there being no end effects for the infinite grating. In the following we will assume that the number of elements $\mathcal{N} = 2N+1$ is very large (but for simplicity retain the condition that $\mathcal{N}b \ll r$) and take advantage of the simplifying feature of the infinite grating by explicitly neglecting end effects and allowing the sums over σ to range from 1 to N . What we are doing essentially is to consider the effects at P of only \mathcal{N} elements of an infinite grating taking into account the contributions to the excitation of each element to all orders of scattering from only its N pairs of nearest neighbors. By this procedure we simplify the problem

considerably but no doubt lose some of the characteristics of the finite grating hinging on the end effects.

On neglecting the end effects, the expressions of (4.10) reduce to

$$(4.16) \quad \psi = H_0 \Delta(\kappa) \left[C + \sum_{n, n', n'' \dots} C_n^S \sum_{m=2}^{\infty} \left\{ \prod_{\mu} C_n^{\mu S} S_{n^{\mu} n^{\mu+1}} \right\} C_n^{(m=1)} \right] ,$$

$$S_{n^{\mu} n^{\mu+1}} = \sum_{\sigma=1}^N H(\sigma) \left\{ e^{-i\sigma A} + (-1)^{n^{\mu} + n^{\mu+1}} e^{i\sigma A} \right\} = S_- + (-1)^{n^{\mu} + n^{\mu+1}} S_+ = \begin{Bmatrix} X \\ Y \end{Bmatrix} ,$$

where S yields $2 \sum H(\sigma) \cos \sigma A \equiv X$ if the indices have even parity, and S yields $-i2 \sum H(\sigma) \sin \sigma A \equiv Y$ for odd parity. Hence for normal incidence, $A = 0$, the multiply scattered orders form a geometrical progression and can be summed explicitly, the product over μ reducing to $(C_e^0 X)^{m-2}$, provided $|C_e^0 X| < 1$. Thus ψ reduces simply to

$$(4.17) \quad \psi = H_0 \Delta(\kappa) \left[C + C_e^1 C_e^0 X / (1 - C_e^0 X) \right] , \quad X = 2 \sum H(\sigma) ,$$

where α is set equal to zero in $\Delta(\kappa)$, C , and C_e^n . (the last of these reducing simply to $\sum \epsilon_n A (-1)^{n/2}$, n even). This expression constitutes the far field of the total wave scattered by a finite grating of identical cylinders, with spacing large compared to wavelength and radius, and width small compared to distance of observation, for a normally incident plane wave, subject to the approximation that the end effects have been neglected. Except for the presence of X , a hitherto untabulated function, this expression is no more difficult to employ for numerical calculations than the solution for the single cylinder.

This expression is valid provided that $|C_e^0 X| < 1$ so that the present approximate series representation of (4.17) converges. Although the mathematical form of (4.17) as such is meaningful for values of the parameters for which $|C_e^0 X| > 1$, and these are not obviously excluded by the physical restrictions imposed on the problem, we will not consider this range because of the difficulty of interpreting (4.17) physically. We will retain the concept of multiple scattering, which apparently hinges on $|C_e^0 X| < 1$, because of its suggestiveness, and also since it seems clear from physical considerations that were we to take into account the absorbing properties of the external medium, the complete series representation of (4.3) would be convergent.

Retaining the concept of multiple scattering it can be seen that the multiply scattered orders are all in phase to reinforce when $\arg(C_e^0 X) = 0$, and that successive multiply scattered orders are 180° out of phase and partially annul each other when the argument equals π . Whether the single scattered value is effected appreciably, however, depends largely on the magnitude of the sum in X (which has its maximum value of $\sum \sigma^{-1/2}$ when $Kb = 2p\pi$, or when the spacing is an integral number of wavelengths so that each multiply scattered order is a maximum), and also on the phase of the second order relative to the first. These conditions cannot in

general be satisfied simultaneously. Thus even were the first and second orders in phase, each order of scattering would be a maximum and all orders in phase only for the special case where Kb equalled $2p\pi$ and $\arg(C_e^0)$ equalled $i\pi/4$ simultaneously. In general, however, because of the particular physical constants of the cylinders, we expect that the greatest effects will be observed when the conditions on the excitations (that they be in phase in each order) and on the orders (that successive orders be in or out of phase) are only partially fulfilled simultaneously.

For arbitrary α the situation is somewhat more complicated. The multiply scattered orders,

$$(4.16') \quad \psi^m = H_0 \Delta(\mathcal{N}) \sum_{n, n', \dots} C_n^I S_{nn'} C_{n'}^O S_{n'n''} C_{n''}^O \dots S_{n(m-2)n(m-1)} C_{n(m-1)}^{C''} , \quad m > 1,$$

do not in general reduce to simple products. We will, however, obtain a closed form representation for the general case by considering four special cases for which the summation procedure is obvious.

Thus if $Y=0$ or $S_-^I = S_+$, only those terms in ψ^m for which the indices of adjacent C 's have even parity are left and we obtain

$$(4.18) \quad \psi^m = H_0 \Delta(\mathcal{N}) \left[C_e^I C_e^I (C_e^O)^{m-2} + C_e^I C_e^{II} (C_e^O)^{m-2} \right] X^{m-1} ,$$

$$\begin{aligned} \psi &= H_0 \Delta(\mathcal{N}) \left[C + C_e^I C_e^I X / (1 - C_e^O X) + C_e^I C_e^{II} X / (1 - C_e^O X) \right] \\ &= H_0 \Delta(\mathcal{N}) \left\{ C + \left[(C_e^I C_e^{II} + C_e^I C_e^I) X - (C_e^I C_e^O C_e^{II} + C_e^I C_e^O C_e^{II}) X^2 \right] / (1 - C_e^O X + C_e^O C_e^O X^2) \right\} . \end{aligned}$$

This obtains physically when $A = Kb \sin \alpha = p'\pi$, where p' is integral, or when the primary excitation of neighboring elements is either in or out of phase. This expression differs from that for normal incidence in possessing the additional component involving the odd single cylinder scattering coefficients. The infinitely many orders of multiple scattering have therefore been reduced to essentially two components, one depending on the even modes of oscillation of the single cylinder, and the other on the odd, which "compete" to determine the character of the effects. Thus a wavelength whose intensity is enhanced for normal incidence may have its intensity reduced for other angles, or conversely. Also the same wavelength may be enhanced in certain of its spectral orders and reduced in others.

Similarly if $X=0$ or $S_- = -S_+$, only those terms in ψ^m for which the indices of adjacent C 's have odd parity are left and we obtain

$$\begin{aligned} (4.18') \quad \psi^m &= H_0 \Delta(\mathcal{N}) (C_e^I C_e^I + C_e^I C_e^{II}) Y (C_e^O C_e^O Y^2)^{m-2}, \quad m \text{ even} , \\ &= H_0 \Delta(\mathcal{N}) (C_e^I C_e^O C_e^I + C_e^I C_e^O C_e^{II}) Y^2 (C_e^O C_e^O Y^2)^{m-2}, \quad m \text{ odd} \\ \psi &= H_0 \Delta(\mathcal{N}) \left\{ C + \left[(C_e^I C_e^{II} + C_e^I C_e^{II}) Y + (C_e^I C_e^O C_e^{II} + C_e^I C_e^O C_e^{II}) Y^2 \right] / (1 - C_e^O C_e^O Y^2) \right\} . \end{aligned}$$

This obtains physically when $Kb(1-\sin\alpha) = -Kb(1+\sin\alpha) + 2p\pi$, or $Kb = p\pi$ where p is integral, or when the path difference between adjacent elements is either an integral or half odd integral number of wavelengths. The competition of the odd and even modes evidenced by (4.18) is absent from this expression.

Two other cases for which the ψ^m can be summed by inspection occur when either $S_+ = 0$, $X = Y$, or $S_- = 0$, $X = -Y$. The physical significance of the first is that only the waves traveling "down" the grating as in Fig. 4.1, or in the direction of the projection of the incident wave normal on the grating, are present; similarly for the second, only the waves traveling up the grating exist. These occur to a high degree of approximation when $Kb(1-\sin\alpha) \approx 2p\pi$, $Kb(1+\sin\alpha) \approx p\pi$, for the first and vice versa for the second. For these cases we obtain

$$\begin{aligned} (4.18^m) \quad \psi^m &= H_0 \Delta(\lambda) \quad C^1 C^m (C^0 S_-)^{m-2} S_- , \\ \psi &= H_0 \Delta(\lambda) \left[C + C^1 C^1 S_- / (1 - C^0 S_-) \right] ; \\ \psi^m &= H_0 \Delta(\lambda) \quad \underline{C}^1 \underline{C}^m (C^0 S_+)^{m-2} S_+ , \\ \psi &= H_0 \Delta(\lambda) \left[C + \underline{C}^1 \underline{C}^1 S_+ / (1 - C^0 S_+) \right] , \end{aligned}$$

where $\underline{C}^1 = \sum C_n^1 (-1)^n = C_e^1 - C_o^1$, and $\underline{C}^m = \sum C_n^m (-1)^n = C_e^m - C_o^m$. (These cases while not particularly realistic for symmetrical elements except for special values of α , may be the more significant ones for gratings with asymmetrical elements or grooves for which pronounced shielding effects may occur in one direction.)

From (4.18) and (4.18') we can construct a function which reduces to either the former or the latter as either Y or X goes to zero. Thus the pertinent quotient can be written as

$$\frac{(C_e^1 C_e^1 + C_o^1 C_o^1)X + (C_e^1 C_o^1 + C_o^1 C_e^1)Y + (C_e^1 C_e^0 C_e^m + C_o^1 C_o^0 C_o^m)(Y^2 - X^2) + G(XY)}{1 - C^0 X + C_e^0 C_o^0 (X^2 - Y^2) + g(XY)} ,$$

where the factors G and g can contain only terms involving products of the form $X^m Y^n$ since these must vanish when either X or Y vanishes. Similarly from (4.18'') we obtain

$$\left[C^1 C^1 S_- + \underline{C}^1 \underline{C}^1 S_+ + F(S_+ S_-) \right] / \left[1 - C^0 (S_+ + S_-) + f(S_+ S_-) \right] ,$$

where F and f involve products of the form $S_+^m S_-^n$.

Each of these quotients is an explicit representation of the sum of the orders of (4.16') provided that the unknown factors are chosen correctly. The correct choice insures that the quotients are identical, and the restrictions on the unknowns provide a means for their determination. It can be seen that the sum of the first two terms of each numerator and each denominator are identical so that the XY repre-

sentation includes all the explicit terms of the other. Furthermore since $x^2 - y^2 = S_+ S_-$, the third terms of the numerator and denominator of the XY representation are in accord with the restrictions on F and f. We establish that F and f contain only these terms, or that G and g are zero from the following consideration. The quantities G and g yield only terms involving $x^m y^n = S_+^{m+n} + S_-^{m+n} \dots$. Were G and g not equal to zero, the presence of the leading terms would contradict the statement of the properties of F and f. Hence G and g are identically zero. (A rigorous proof will be found in the appendix)

We therefore obtain for arbitrary α the closed form representation of the total scattered wave*

$$(4.19) \psi = H_0 \Delta(\alpha) \left\{ C + \frac{(C'_e C''_e + C'_o C''_o)X + (C'_e C''_o + C'_o C''_e)Y + (C'_e C''_e C''_o + C'_o C''_o C''_e)(Y^2 - X^2)}{1 - C^o X + C^o C^o (X^2 - Y^2)} \right\},$$

or

$$(4.19') \psi = H_0 \Delta(\alpha) \left\{ C + \frac{C' C'' S_- + C' C'' S_+ - [C' (C^o C'' - C^o C'') + C' (C^o C'' - C^o C')] S_- S_+}{1 - C^o (S_- + S_+) + [(C^o)^2 - (C^o)^2] S_- S_+} \right\}.$$

The interpretation of the quotient of (4.19') is as follows; the factors C' and C'' , or the single cylinder factor $\sum \epsilon_n A_n \cos n(\theta + \alpha) = C$ with $\alpha = \pm \pi/2$, indicate that the quotient consists essentially of two outgoing waves arising from the excitations incident on each cylinder in the plane of the grating. The factors C^o and C^o , or C with $\theta = \pm \pi/2$ that each of these waves contains indicate that the excitations arise from the waves scattered by the cylinders in the plane of the grating. The presence of C^o and C^o , or C with $\theta + \alpha = 0$ or π , the forward and back scattered single cylinder factors, merely indicates the effects of intervening cylinders. (See section 3.2 for a fuller discussion for two cylinders.)

For an infinite grating the solution would be of the same form as the above but more rigorous in that there would be no need to neglect the end effects. Thus we obtain

$$(4.19'') \psi = \sum_{s=-\infty}^{\infty} H_0(r_s) e^{-isA} \sum_n e^{in\theta_s} \left\{ e^{in\alpha} + \frac{i^n S_- [C'' - (C^o C'' - C^o C'') S_+] + i^{-n} S_+ [C' (C^o C'' - C^o C'') S_-]}{1 - C^o (S_- + S_+) + [(C^o)^2 - (C^o)^2] S_- S_+} \right\}$$

where the limits on S_{\pm} are 1 and ∞ . Various techniques have been developed to

* Originally the writer had considered only the explicit forms of (4.17, 18, 18', 18''), particularly (4.18) which obtains for maximal effects. Expression (4.19) was obtained after Dr. S. Karp, who is investigating the grating of arbitrary identical elements by means of integral equations, showed that the explicit representation for arbitrary α should be essentially of the same form as these special cases; the writer is grateful to Dr. Karp. Solution of the simultaneous equations he obtained for the charge distribution on an arbitrary element no doubt lead to (4.19'') when specialized for cylindrical elements.

approximate the sums involved, but we will not discuss this case since we believe that the finite grating, albeit with end effects neglected, is a better model for the laboratory equipment usually employed. Furthermore, for the wavelengths of (4.12') or the range of particular interest, the sums in S_{\pm} would not converge, our closed form representation would not be valid, and in its expanded form the solution would predict infinite intensity for these wavelengths. Rayleigh's treatment of an infinite grating⁷, although quite different from our own, also indicated the intensity would become infinite for these wavelengths. While this might account for the maxima observed, it would not account for the minima, nor, more significantly, for the fact that the most pronounced parts of the "anomalies" were observed at slightly different wavelengths, their displacement depending on the substance of the grating. It will be shown in the following sections that the present theory of the finite grating is adequate to account not only for these phenomena but also for the others that have been observed.

4.3 Mode Approximations

To facilitate future discussion and to derive approximate solutions which can be readily analyzed, we will restrict the parameters so that $x \rightarrow 0$, where $x = Ka$ or Ka' , thus limiting the discussion to cylinders with radii very small compared to wavelength, or with larger radii provided that the dielectric constant or index of refraction of the cylinders differs little from that of the external medium.

There are essentially two procedures for approximating our solution; either we expand it in a power series in x and retain only the terms to a specified power, or else we retain only the leading terms in x in all orders of scattering. To illustrate the first procedure, a solution to powers in x^4 is obtained by retaining only the terms in A_0 , A_1 and A_2 in ψ^1 , and the terms in A_0^2 , A_1^2 , A_0A_1 in ψ^2 and neglecting all other terms and all higher orders of scattering. However, because of the rapid increase of the number of terms in each power of x with increasing m , the sum of the remaining terms may well be of the same order of magnitude or larger than the terms retained.

The alternate procedure, and the one we will follow, is based on the fact that the A_n correspond to the modes of oscillation of the single cylinder. Thus, for example, if we assume that each cylinder can oscillate only in the " A_0 mode", or that each scatters isotropically regardless of the wave form of the incident radiation, we would retain only the terms containing A_0 in all orders of scattering. (Essentially this sort of assumption was tacit in most previous work on multiple scattering.) This assumption seems physically plausible for certain ranges of the parameters, but it is apparent from our expressions that by its use we introduce discrepancies as to the powers of x retained (in addition to those in K_0 introduced by the use of the asymptotic form of the H 's mentioned previously). We note that

for the present problem the discrepancies should, in general, prove much less significant than for the problem of two cylinders. Thus while we may retain the terms to x^4 in ψ^2 and only those to x^2 in ψ^1 , the terms in ψ^2 are multiplied by X which is in general much larger than unity; similarly for the higher orders. The virtue of this procedure, which is employed primarily for heuristic purposes, is that all orders of scattering are retained, albeit only the largest terms of each, to yield physically plausible explicit solutions which can be analyzed with a minimum of numerical computations.

Retaining only A_0 and A_1 in all orders yields

$$(4.20) \quad \psi = H_0 \Delta(\mathcal{N}) \left\{ A_0 + 2A_1 \cos(\theta + \alpha) + \frac{(A_0^2 - 4A_1^2 \sin\theta \sin\alpha)X + 2A_0 A_1 [(\sin\alpha - \sin\theta)Y + (A_0 - 2A_1 \sin\theta \sin\alpha)(Y^2 - X^2)]}{1 - (A_0 + 2A_1)X + 2A_0 A_1 (X^2 - Y^2)} \right\}.$$

The second order of scattering of the above equals

$$(4.21) \quad \psi^2 = H_0 \Delta(\mathcal{N}) \left[(A_0^2 - 4A_1^2 \sin\theta \sin\alpha)X + 2A_0 A_1 (\sin\alpha - \sin\theta)Y \right].$$

Had we not neglected the end effects we would have obtained an expression for ψ^2 formally identical but with $\Delta(\mathcal{N})X$ and $\Delta(\mathcal{N})Y$ replaced by

$$(4.21') \quad \Delta(\mathcal{N}) \begin{Bmatrix} X \\ Y \end{Bmatrix} = 2 \sum_{s=-N}^{N-1} \sum_{\sigma=1}^{N-s} H(\sigma) \begin{Bmatrix} \cos \\ -i \sin \end{Bmatrix} (s\gamma + \sigma A) = 2 \sum_{\sigma=1}^{2N} \Delta(\mathcal{N} - \sigma) \begin{Bmatrix} \cos \\ i \sin \end{Bmatrix} (\sigma\gamma'/2).$$

We will employ this result shortly to compare the magnitudes of ψ^2 for end effects neglected and retained. The "modes", A_0 , A_1 , and $A_0 + A_1$, will be considered.

4.31 " A_0 mode": Isotropic Scatterers

For an incident plane wave polarized parallel to a cylinder's axis, or for a cylinder of zero impedance in acoustics, and $Ka \rightarrow 0$, the largest coefficient is $A_0 = iB_0 e^{i\phi}$, where B_0 and ϕ are real and positive as in (1.60, 61, 63). Invoking the mode hypothesis yields

$$(4.22) \quad \psi^1 = \Delta(\mathcal{N}) H_0 A_0, \quad \psi^m = \Delta(\mathcal{N}) H_0 A_0^m X^{m-1}.$$

Summing the various orders for $|A_0 X|^2 < 1$ we obtain the total scattered wave

$$(4.23) \quad \psi = \sum \psi^m = \psi^1 / (1 - A_0 X), \quad X = 2 \sum H(\sigma) \cos \sigma A,$$

which is valid for all angles of incidence. We will first investigate the range of validity of the usual single scattering approximation and then go on to the maximal effects of multiple scattering.

An analytic criterion for the range of validity of the single scattering hypothesis is that the sum of the multiply scattered orders be small compared to the total scattered wave, or that

$$(4.24) \quad B = |(\psi - \psi^1)/\psi| = |A_0 X| = B_0 2t(2/\pi Kb)^{1/2} \ll 1,$$

where t is defined by

$$(4.25) \quad t e^{i\gamma} = \sum \sigma^{-1/2} e^{i\sigma Kb} \cos(\sigma Kb \sin \alpha) = T,$$

T being essentially the sum analogue of the integral yielding the Cornu spiral. We note that for the present problem B is also identically $|\psi^2/\psi^1|$. For cases where it is not possible to sum ψ explicitly but where ψ^2 can be readily obtained (e.g., when the end effects are retained), we would also employ $|\psi^2/\psi^1| \ll 1$ as a criterion for single scattering theory since if $|\psi^2| \ll |\psi^1|$, it follows that $|\psi^3| \ll |\psi^2|$, etc. It can be seen that the criterion for this case, or $|A_0 X| \ll 1$, could have been obtained simply by noting that the single scattering solution for the grating on neglecting the end effects is $A_0 X$ when evaluated at any of the cylinders. The wave each cylinder scatters in response is then proportional to this excitation factor so that the smallness of the factor would insure that the second order wave scattered by the cylinder is negligible; similarly for the higher orders. This same sort of approach could have been employed to write down (4.23) immediately, i.e., the excitation of each cylinder in each order is simply a multiple of $A_0 X$ so that the wave it scatters is its single scattered wave times this quantity, etc.

The quantity B of (4.24) differs from that obtained for two cylinders in possessing the additional factor $2t$. Employing the maximum value of t , or $\sum_{\sigma=1}^N \sigma^{-1/2}$, for an inclusive criterion yields, for example, $2t \approx 26$ for $N = 50$

indicating a much more limited range of validity than for the two cylinders.

Had we employed $|\psi^2/\psi^1|$, with ψ^2 as obtained with (4.21), taking the end effects into account, the maximum value of t would be $N^{-1} \sum_{\sigma=1}^{2N} (N-\sigma) \sigma^{-1/2}$ or $2t \approx 24$ for

$N = 50$. The difference of the two quantities is negligible for our present purpose, although significant differences may arise for other applications. These values of t indicate that the numerical values of Kb and x' employed in (3.46) to obtain $B < 5\%$ for two cylinders now yield that the first and second order waves

are of the same order of magnitude. Thus for the perfect conductor, $B_0 = \pi/2 \ln(2/\gamma x)$, we now require $b/\lambda \approx 9 \times 10^4$, 6×10^3 , 2×10^3 for $x = 0.5$, 0.05 , 0.005 respectively, to insure that $B < 5\%$. Similarly for the dielectric, $B_0 = \pi x'^2/4$, where for two cylinders $x' = 0.3$, $\lambda/b \approx 1$ sufficed, we now require $\lambda/b \approx 600$ for the same value of x' , or $x' \approx 0.06$ for the same value of λ/b to insure that $B < 5\%$. For larger values of N the effects of multiple scattering become even more pronounced. Thus for $N = 5000$ we obtain $2t \approx 280$ (or $2t \approx 260$ on taking into account the end effects) requiring much smaller values of Ka and much larger values of Kb for single scattering theory to be valid.

The minimum values of t , corresponding to the minimal wavelengths of (4.14), are $\sum_{n=1}^N (-1)^n \sigma^{-1/2}$ when the end effects are neglected and $N^{-1} \sum_{n=1}^{2N} (N-\sigma)(-1)^n \sigma^{-1/2}$ when they are taken into account. For $N = 50$ or larger both yield $2t \approx 1$ so that the effects are only of the same order of magnitude as for two cylinders and are, in general, negligible.

4.311 Qualitative Analysis of the Solution

We will now investigate the behavior of ψ to determine the character of the maximal effects, or the extrema of $R = |\psi/\psi^1|^2$, and their dependence on the various parameters of the problem. Since it is not feasible to determine these extrema mathematically, and because of the lack of tabulated values of T (this function not having been investigated to the writer's knowledge), we will first show that the most interesting features of the intensity curves, R vs. λ , can be deduced from elementary physical considerations, and then in section 4.312 substantiate these by numerical computations. We follow this procedure since we are primarily interested in deriving general, if approximate, relations for the positions of the peaks of the anomalies discovered by Wood⁴, their dependence on the physical constants of the grating, the wavelength, etc., rather than in merely considering a few numerical exercises.

We rewrite (4.23) as

$$(4.26) \quad \psi = \psi^1 / (1 - B e^{i\beta}) = \psi^1 [1 + B e^{i\beta} + (B e^{i\beta})^2 \dots],$$

where $B = |A_0 X|$ as in (4.24) and where

$$(4.27) \quad \beta = \gamma + \phi + \pi/4 = \arg(T) + \arg(A_0 i^{-1/2})$$

is the phase difference of successive orders. From elementary considerations we

expect maximal effects of multiple scattering yielding intensity maxima for wavelengths which insure that each order of scattering is a maximum and all orders of scattering are in phase. The first condition, requiring that all excitations in each order are in phase, is met by the wavelengths of (4.12) which yield $\gamma = 0$, $T = t = 2 \sum \sigma^{-1/2}$, while the second requires that

$$(4.28) \quad \beta = 2n\pi, \quad n = 0, 1, 2, \dots, \quad \text{and yields } \psi = \psi^1/(1-B),$$

where B contains the maximum value of t. However, these conditions on γ and β can be satisfied simultaneously only when $\phi + \pi/4 = 2m\pi$, which is a rather special and unrealistic case. More generally, for the usual physical substances employed, no wavelengths will satisfy both conditions simultaneously. Hence whether or not pronounced maxima are observed is governed largely by the physical substance of the grating, since it is evident that either condition by itself will not insure maximum scattering.

Thus in general, it is clear that merely requiring that all orders of scattering be in phase, and their graph in the complex plane a straight line, may not necessarily yield maximum scattering since the graph of the excitations may "spiral" and the magnitudes of the individual orders of scattering be small; the extreme case of this is the minimal case (4.14) mentioned previously. Another example is illustrated in Fig. 4.3a which is a graph of T in the complex plane for $Kb(1 \pm \sin \alpha) = 2p_{\pm}\pi + \pi/2$, excitations of each cylinder reaching it from pairs of successive neighboring cylinders (or "successive excitations") being 90° out of phase. It can be seen that although the phase of the resultant, γ , is roughly 125° so that (4.28) is approximately satisfied for $\phi = \pi$ (for a perfect conductor), the effects are slight since the magnitude of the resultant, t, is less than that of the leading term of the series. Similarly for the reverse of this situation, although

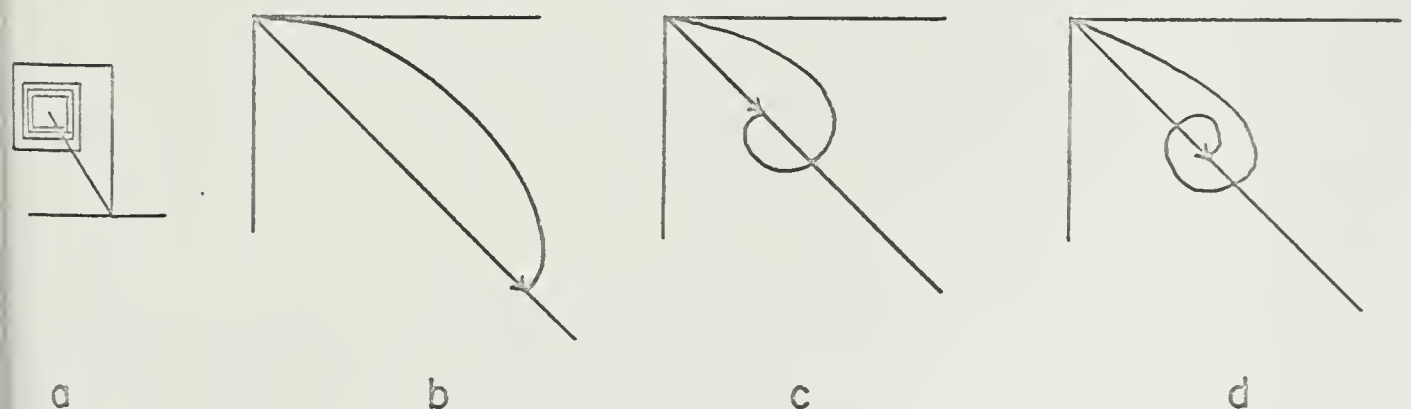


Fig. 4.3

all excitations in each order may be in phase and their graph a straight line, the graph of the orders of scattering may spiral and the total scattering be small; in fact if successive orders are out of phase or

$$(4.29) \quad \beta = (2n+1)\pi, \quad \psi = \psi^1/(1+B),$$

and the resultant of the excitations large, we obtain maximal effects yielding a minimum of the total scattered wave. Hence, in general, the conditions on the excitations and the orders can be satisfied only partially, the maximal effects arising from their optimal fulfillment.

The graphs of T in the complex plane for the largest values of t for $\gamma = -\pi/4$, satisfying (4.28, 29) for $\phi = 0, \pi$ respectively, are sketched in Fig. 4.3b,c,d for N very large. The largest of these values of t occurs when the phase difference of successive excitations, say δ , is sufficiently small so that the graph approximates a "simple arc" as in Fig. 4.3b. This value of δ , say δ' , yields the extrema of $(1 \mp B)^{-1}$ which contain the largest value of t commensurate with the prescribed phase corresponding to an intensity decrease for the perfect conductor, $\phi = \pi$, and an intensity increase for the perfect dielectric, $\phi = 0$. We expect, however, that the maximal effects will occur for a smaller value of $|\delta|$, say δ_{\wedge} lying between 0 and δ' , or when the excitations are more nearly in phase than is required by (4.28,29); i.e., $\delta = 0$ satisfies (4.12), while $\delta = \delta'$ satisfies (4.28,29), neither by itself yields the maximal effects, which occur rather for, say, $\delta_{\wedge} \approx \delta'/2$, as a rough figure of merit.

We obtain an approximate upper limit or figure of merit for δ' , in terms of N and ϕ , from the following considerations.* The largest value of t with a phase of -45° (or for $\phi = 0, \pi$) occurs when the graph of the excitations is still a simple arc as in graph b. For this simple arc case to obtain, we require that the last vector, or N -th excitation, makes an angle less than 90° with the resultant, since if this angle is greater than 90° the graph has already begun to "spiral" to assume the form of graph c and the resultant to decrease. Hence for the largest value of t commensurate with $\gamma = -45^\circ$ we have $|N\delta| \leq \pi/4 + \pi/2$. (In general, $|N\delta| \leq |\gamma| + \pi/2$ where $|\gamma|$, as prescribed by (4.28,29), equals $\phi + \pi/4$ for the maxima and $\pi + \phi + \pi/4$ for the minima.) Although this procedure lays no claim to rigor we can accept $|\delta'| \approx 3\pi/4N$ as a convenient figure of merit. The most interesting feature of this result is the fact that δ' depends only on N , the number of nearest neighbors we take into account, and on ϕ , the phase of the scattering coefficient of the single cylinder, and is apparently independent of the remaining parameters of the problem. Now since the maximal value δ_{\wedge} does not differ greatly from δ' , we accept as a working hypothesis that δ_{\wedge} also depends primarily on N and ϕ and is essentially independent of the

* The writer is indebted to Prof. W. Magnus for suggesting this.

other parameters. (This is verified by numerical computations in the next section.) Hence the greatest effects, decreasing the intensity for the perfect conductor and increasing it for the perfect dielectric, occur for the maximal values

$$(4.30) \quad K_{\Delta} b (1 \pm \sin \alpha) = 2p_{\pm} \pi + \delta_{\Delta}, \quad T_{\Delta} = \sum \sigma^{-1/2} e^{i\sigma \delta_{\Delta}},$$

where δ_{Δ} is a small negative quantity between 0 and $-3\pi/4N$. On the basis of this expression the more interesting features of the intensity curves can be obtained immediately.

On writing $K_{\Delta} b = K_0 b + \delta_{\Delta}$, where K_0 corresponds to the wavelengths for $\delta = 0$, we obtain for the displacement of the maximal wavelengths from the values of (4.12)

$$(4.31) \quad \Delta_{\Delta} = \lambda_{\Delta} - \lambda_0 = -\delta_{\Delta} \lambda_0 / 2\pi b \approx |\delta_{\Delta}| \lambda_0^2 / 2\pi b = |\delta_{\Delta}| b / 2\pi p^2 < 3\lambda_0^2 / 8\pi b.$$

This indicates that the maximal effects are "shifted to the red", or occur on the long wavelength side of the wavelengths $\lambda_0 = b/p$, the displacement being roughly proportional to λ_0^2 / Nb , or to the square of the wavelength divided by the width of the grating. (For the conducting dielectric, $\Delta_{\Delta} < (\phi + 3\pi/4) / 2\pi bN$.) On the basis of the above and the preceding discussion it can be seen that the most pronounced effects of multiple scattering cover a finite portion of the λ -axis, and form a "maximal band" whose "peak" is at $\lambda_{\Delta} > \lambda_0$; this agrees with the experiments of references 4, 5, and 6. The width of the band is essentially proportional to Δ_{Δ} so that the ratio of the band widths for different λ_{Δ} 's, the other parameters being fixed, is approximately

$$(4.32) \quad w_p / w_{p+1} = w \approx (p+1)^2 / p^2.$$

Thus for $p = 3$ we find $w \approx 1.8$ so that the band in the vicinity of $\lambda_0 = b/3$ should be almost twice as wide as that occurring near $\lambda_0 = b/4$. (This agrees with the spectrograms for normal incidence obtained by Wood, reference 4, Fig. 1, 1935.)

For white light, or any other broad band radiation, incident on the grating we expect that the intensities of these bands will be less than their single scattered values, or dark relative to neighboring wavelengths, if the elements are perfectly conducting, and bright if the elements are perfect dielectrics. It is evident from Fig. 4.3c and d, however, that these bands are not simple intensity extrema (as for two cylinders), but that they are flanked, at least on the long wavelength side, by a succession of "local extrema" which become less pronounced as $|\delta|$ increases.

From Fig. 4.3 we can deduce the form of the curve of $R = |\psi/\psi^1|^2 = |(1 - Be^{i\beta})|^{-2}$ vs. λ , or R vs. $-\delta$. Thus for the perfect conductor, as λ increases, the curve passes through a deep minimum indicated by graph b, rises to a low local maximum with P still less than unity indicated by graph c, and falls to another minimum not as low as the first as indicated by graph d. With increasing λ the values of these

local extrema approach unity, or $\psi \rightarrow \psi^1$, as λ approaches its minimal value, or $\delta \rightarrow \pi$. The approximate positions of these local extrema are obtained by adding multiples of π/N to that for the maximal value. Thus we have $N\delta' \approx -\pi/4 - (2n-1)\pi/2$, the odd values of n corresponding to the minima, and the even to the maxima. The maximum value of n corresponds to the minimal region, or $\delta = \pi$, so that the number of extrema is of the order of the number of pairs of cylinders. Only the first few extrema should be significant, however, because of the behavior of T with increasing δ_0 . It can be deduced that T has the spiral form indicated by d , until $\delta = \pi/2$ is reached, and that thereafter the graph becomes a jagged "star patch" with a rapidly decreasing resultant.

For the perfect dielectric the situation is essentially as above and its discussion requires merely the interchange of the words maximum and minimum, high for low, etc., to be fully applicable.

Another significant point of the behavior of the R - λ curve that can be established without numerical calculation is that the sharp boundary of the peak occurs on its short wavelength side. Thus the derivative of $R = |\psi/\psi^1|^2$ with respect to wave number is $\partial R/\partial K = -R^2 \left\{ -2D' \sum \sigma^{-1/2} \cos(\sigma Kb + \phi + \pi/4) + 2D \sum \sigma^{1/2} \sin(\sigma Kb + \phi + \pi/4) + (D^2)' \sum \sum (\sigma\sigma')^{-1/2} \cos(\sigma - \sigma') Kb - D^2 \sum \sum (\sigma\sigma')^{-1/2} (\sigma - \sigma') \sin(\sigma - \sigma') Kb \right\}$, where $D = 2B_0(2/\pi Kb)^{1/2}$ and $D' = \partial D/\partial K$. Substituting $Kb = 2\pi$, $\delta = 0$, yields $\partial R/\partial K = -R^2 \left\{ -2D' \cos(\phi + \pi/4) \sum \sigma^{-1/2} + 2D \sin(\phi + \pi/4) \sum \sigma^{1/2} + (D^2)' (\sum \sigma^{-1/2})^2 \right\}$. Retaining only the largest term, $-R^2 2D \sin(\phi + \pi/4) \sum \sigma^{1/2}$, since $\sum \sigma^{1/2} \gg \sum \sigma^{-1/2}$ and $K \gg 1$, we see that the slope of the R - λ curve, $\partial R/\partial \lambda = -(K^2/2\pi) \partial R/\partial K$, is very large in the immediate vicinity of λ_0 . Thus for the perfect conductor, $\phi = \pi$, and $\partial R/\partial \lambda$ is negative indicating that the intensity drops sharply in the vicinity of λ_0 , while for the perfect dielectric $\phi = 0$ and $\partial R/\partial \lambda$ is positive indicating a sharp intensity rise. (The sharp boundary at λ_0 agrees with the previously mentioned experiments.)

So far we have considered only $\lambda > \lambda_0$, or $\delta = -|\delta|$, but there is no basis for assuming that departures from single scattering theory cannot occur for $\lambda < \lambda_0$. Were it possible for the graph of T in the complex plane to assume the shapes in Fig. 4.4 below, to yield $\psi = 3\pi/4$ satisfying (4.28,29), the situation would be analogous to the previous, except that the character of the anomaly for the particular substance would be reversed. Furthermore, since the δ 's are larger and positive the maximal effects and local extrema would be shifted more to the blue than the previous were to the red, the most pronounced extrema occurring in the vicinity of $\delta \approx 5\pi/4N$ as in sketch a and yielding a band of opposite character to that at $\lambda_0 + \Delta_\lambda$. In general the extrema would occur for $N\delta \approx \pi/4 + n\pi$, so that the values of $\lambda < \lambda_0$ at which the local extrema occur interlace those for $\lambda > \lambda_0$.

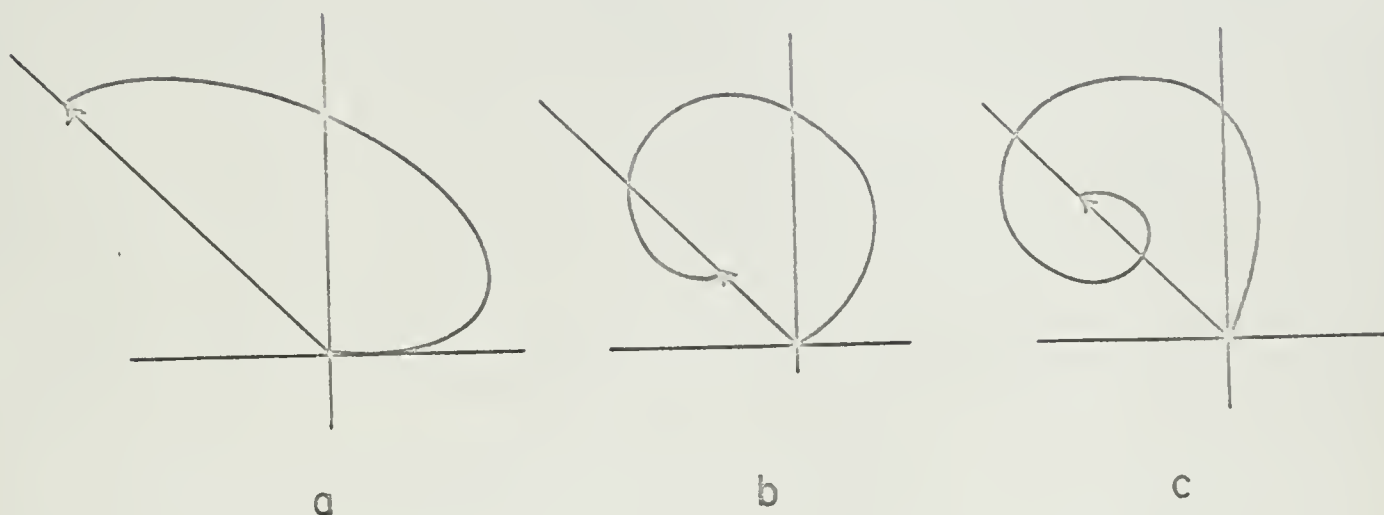


Fig. 4.4

It can be deduced from Fig. 4.3a, however, that for $\gamma = 3\pi/4$ the resultants of the graphs are very small, T falling in the "star patch" region mentioned previously, so that the corresponding values of δ are actually greater than $\pi/2$ and are not in the vicinity of λ_0 at all. The values of $\delta' = (\pi/4 + n\pi)/N$, since they interlace the previous negative values, correspond to graphs and resultants as indicated in Fig. 4.5, the last vector being more or less parallel to $\gamma = 45^\circ$ for all cases.

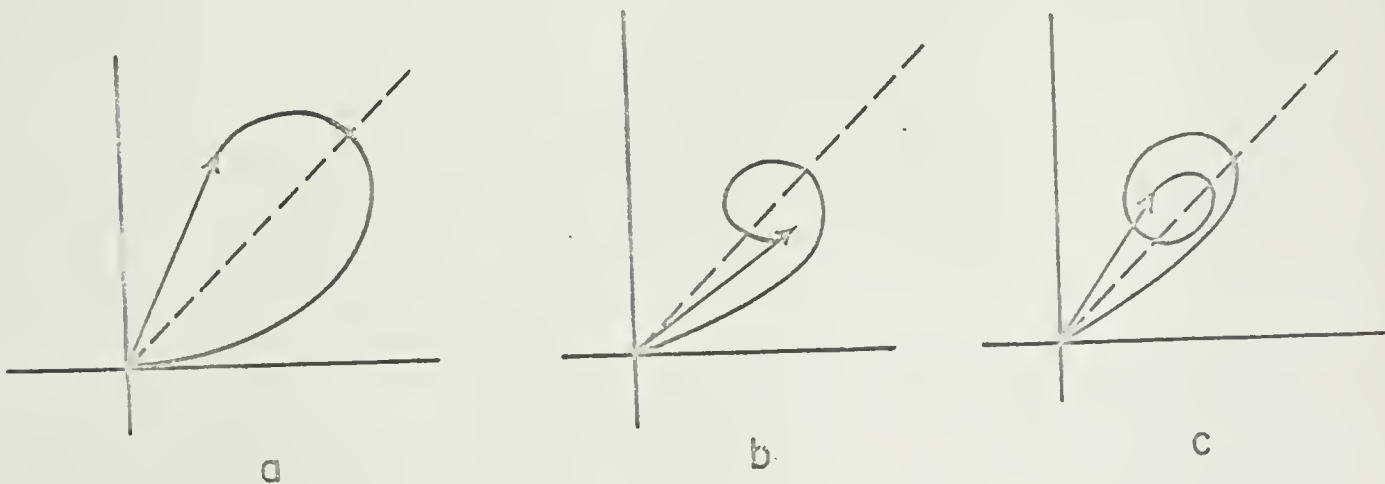


Fig. 4.5

It is not obvious from these figures and the form of ψ that these values of δ and γ correspond to local extrema of opposite character to those obtained from Fig. 4.5. Although the periodicity of these effects is identical with that obtained from the graphs of Fig. 4.4, the values of γ of Fig. 4.5 do not satisfy (4.28) so that these local extrema (if they occur) occur when successive orders of scattering are neither approximately in or out of phase and are as a consequence not as pronounced as the previous. It is conceivable, however that the magnitudes and phases of the orders may be such as to yield appreciable departures of R from unity but this can only be determined by numerical calculations. We are loath to discard these values of δ' as extremal values because of the physical plausibility of the complementary and interlacing effects they predict on the short wavelength side of λ_0 ; the complementary character of these bands is precisely what is required to obviate questions as to the conservation of energy in the multiple scattering process.

We return now to consideration of the maximal band, to obtain some idea of its angular width. We take as a figure of merit the range bounded by λ_0 and the first local extremum on its long wavelength side, or for simplicity $W = b/Np^2$ which should be correct to within a factor of 2. For normal incidence the angular positions of the λ_0 's are given by $\sin\theta = q/p = q\lambda_0/b$. Hence $\Delta(\sin\theta) = q\Delta\lambda_0/b$, or for relatively small values of θ , $\Delta\theta \approx qW/b = q/Np^2$. Thus the maximal band is quite narrow, subtending only a small fraction of a degree, even for only moderately large values of N ; e.g., for $q = 1$, $p = 3$, and $N = 10, 10^2, 10^3, 10^4$ we obtain $\Delta\theta \approx 40', 4', 0.4', 0.04'$ respectively. In general we have $\Delta\theta = q/Np^2 \cos\theta = q\lambda_0/bpN\cos\theta$ which for $\lambda \approx 2N$ is of the same order of magnitude as $\lambda_0/\lambda b \cos\theta$, the angular half width of a principal maximum of $\Delta(\lambda)$. It can be seen that if all parameters but α and θ are held constant (the bands occurring for $\sin\alpha = p'/p$, $\sin\theta_0 = (q-p')/p$, $p' = 0, 1, 2, \dots, p$), then as α increases, θ decreases and $\Delta\theta$ or the band width should decrease. (See Wood⁴, 1935, Fig. 1.3, where this decrease occurs but more rapidly than if due solely to a $\sec\theta$ effect.)

The resolving power for the maximal band is $\lambda/\Delta \approx pN$, or of the same order of magnitude as $q\lambda$ for a principal maximum of $\Delta(\lambda)$. These results imply that for a discrete source, multiple scattering may have marked effects on one of two closely neighboring lines without effecting the other appreciably. (This was observed by Wood⁴, 1902 with the sodium D lines having a separation of $6A^\circ$ or $\lambda/\Delta \approx 10^3$.) It should be kept in mind that although N is proportional to λ , the number of elements, it is not necessarily of the same order of magnitude, particularly for gratings with more complicated elements for which shielding effects arise, or when absorption in the external medium is significant. These present relations, however, when correlated with experimental measurements of the widths of the peaks and their displacement from

λ_0 should provide a good indication of the value of N for a particular grating.

From the form of the scattering coefficients of the single cylinder appearing in ψ we can deduce the relative intensities of the bands in different parts of the spectrum in the vicinity of different λ_0 's. Thus for the perfect conductor we have $B = t/p^{1/2} \ln(2/\gamma x) \propto \lambda^{1/2} / \ln(\lambda/\gamma a \pi)$ so that subject to the assumption that δ_\wedge , and consequently t_\wedge , is independent of the wavelength we see that B increases as λ increases, the effect of the square root overshadowing that of the logarithm. Hence the bands should depart more from their single scattered values for the longer wavelengths. However, these are not necessarily the darkest bands since the total as well as the single scattered intensity (rather than their ratio) increase as $\lambda / \ln^2(\lambda/\gamma a \pi)$. The least intense bands (or lowest values of $|\psi|^2$) may therefore occur for the shorter wavelengths, while the most pronounced (or lowest values of R) should occur for the longer wavelengths.

For the perfect dielectric we have $B = x'^2 t / 2p^{1/2} \propto \lambda^{-3/2}$, or B increases rapidly with decreasing wavelength. Hence the largest values of R occur for the shorter wavelengths and these bands are also the brightest since $|\psi|^2 \propto \lambda^{-3}$. For the conducting dielectric the situation is essentially as for the perfect dielectric, but since for this case ϕ is usually between 0 and $\pi/2$ we expect that δ_\wedge will be somewhat larger (corresponding to the larger values of γ prescribed by (4.28)). Consequently the maximal effects occur for longer wavelengths and are less pronounced than for the perfect dielectric.

It can also be seen that the brightest bands may have intensities many times their single scattered values, while the least intensity of the dark band is only of the order of one-fourth its single scattered value. This is merely a physical consequence of the fact that all orders reinforce the first for the maximum, while there is only a partial annulment for the minimum resulting from successive orders being approximately out of phase. This is of course evident from ψ of (4.29) and the condition that $B_{\max}^2 < 1$ to insure convergence.

We have for simplicity confined ourselves to this point to the bands for which $A = Kb \sin \alpha = 2p'\pi$ occurring in the vicinity of and displaced to the lower left of the intersections of the heavy lines in Fig. 4.2. In the figure these occur at $\lambda_0 = b/p$, $\sin \alpha = p'/p$, whereas the ones we considered fall at longer wavelengths, $\lambda_\wedge = \lambda_0 + \lambda_\wedge$, and at very slightly larger angles, $\sin \alpha = 2p'\pi / (2p\pi + \delta_\wedge)$. The discussion will now be extended to the partial maximal effects corresponding to the heavy lines of Fig. 4.2 in the vicinity of either λ^+ or λ^- of (4.12').

We write $2T = T_+ + T_- = t_+ e^{i\gamma_+} + t_- e^{i\gamma_-} = \sum \sigma^{-1/2} \left\{ e^{i\sigma(1+A)}_+ + e^{i\sigma(1-A)}_- \right\}$ and obtain in analogy to (4.26) and (4.28)

$$(4.33) \quad \psi = \psi^1 / (1 - B_+ e^{i\beta_+} - B_- e^{i\beta_-}), \text{ and } (4.34) \quad \beta_{\pm} = 2n_{\pm}\pi, = (2n_{\pm}+1)\pi,$$

where $B_{\pm} = B_0 (2/Kb\pi)^{1/2} t_{\pm}$ and $\beta_{\pm} = \phi + \gamma_{\pm} + \pi/4$. Thus if $\beta_+ = 2n_+\pi$ while β_- is arbitrary we expect the scattering to be increased, while if $\beta_+ = (2n_++1)\pi$ we expect it to be decreased. For wavelengths in the vicinity of K^+ we write

$$(4.35) \quad Kb(1+\sin\alpha) = 2p_+\pi + \delta^+ = K^+b(1+\sin\alpha) + \delta^+, \\ Kb(1-\sin\alpha) = (2p_+\pi + \delta^+)(1-\sin\alpha)/(1+\sin\alpha),$$

where we have omitted the maximal symbol, \wedge , for brevity, and obtain

$$(4.36) \quad 2T = \sum \sigma^{-1/2} \left\{ \exp(i\sigma\delta^+) + \exp \left[i\sigma(2p_+\pi + \delta^+)(1-\sin\alpha)/(1+\sin\alpha) \right] \right\},$$

which reduces to $2T$ as in (4.30) for $Kb\sin\alpha = 2p'\pi$, $\delta_{\wedge} = \delta^+ = \delta^-$. Similarly for the vicinity of K^- , we replace \pm by \mp in the above. It can be seen that in general the effects are now dependent on the wavelength and angles of incidence, which are explicit parameters of the terms on the right corresponding to the excitations traveling in the negative y direction. Thus if $Kb(1-\sin\alpha)$ differs appreciably from $2p\pi$ the contribution of T_- are small and B is of the order of half the value it has at the intersections, while if $Kb(1-\sin\alpha) \approx 2p\pi$ the effects are essentially as for the intersections.

For the shift of the peak effects to longer wavelengths corresponding to

(4.31) we now have,

$$(4.37) \quad \Delta_{\pm} = \lambda_{\wedge} - \lambda^{\pm} = -\delta^{\pm} \lambda_{\wedge} \lambda^{\pm} / 2\pi b(1 \pm \sin\alpha).$$

We note that for the case treated previously, $A = 2p'\pi$, although $\delta^{\pm} = \delta_{\wedge}$, the peak values corresponding to λ^+ and λ^- were displaced by different amounts in order for them to coincide at $\lambda = \lambda_0 + \Delta_{\wedge}$; i.e., $\Delta_+ \neq \Delta_- \neq \Delta_{\wedge}$ so that for a given value of α the intersection at $A = 2p'\pi$ arises for $\lambda^+ \neq \lambda^-$. The peaks corresponding to the intersections of the heavy lines of Fig. 4.2, $\lambda^+ = \lambda^- = \lambda_0$, $\sin\alpha = (p_+ - p_-)/(p_+ + p_-)$, $A \neq 2p'\pi$, are shifted by $\Delta_{+\wedge} = \Delta_{-\wedge} = \Delta_{0\wedge}$ but $\delta^+ \neq \delta^-$ and there is no displacement in α . Hence for $Kb(1 \pm \sin\alpha) = 2p_{\pm}\pi + \delta^{\pm} = K^{\pm}b(1 \pm \sin\alpha) + \delta^{\pm}$, $K^{\pm} = K_0$, we have $\Delta_{\pm} = \Delta_0 = -\delta_0 \lambda_{\wedge} \lambda_0 / 2\pi b$, $\delta_0 = \delta^{\pm} / (1 \pm \sin\alpha)$. These quantities Δ_0 , δ_0 should not be confused with those occurring for $A = 2p'\pi$ or those of (4.12), although the values of λ and α at which the two effects occur are practically identical, as are no doubt their intensities and structure. We note that for the present case we have $2Kb = 2\pi(p_+ + p_-) + \delta^+ + \delta^- = 2K_0b + 2\delta_0$, formally analogous to the previous, but that $2Kb\sin\alpha = 2\pi(p_+ + p_-) + \delta^+ + \delta^- = 4p'\pi + 2\delta_0 \sin\alpha$. This differs from the previous by the $\delta_0 \sin\alpha$ term whose presence indicates that we are investigating the effects at the same value of α at which λ_0 occurs rather than at a larger value of α as for the previous case.

Introducing $\delta^\pm = \delta_0(1 \pm \sin \alpha)$, which is a general relation, into (4.37) and assuming as for the previous δ_\wedge that δ_0 is independent of the wavelength yields for the partial maximal effects

$$(4.37') \quad \Delta_\pm = -\delta_0 \lambda \wedge \lambda^\pm / 2\pi b \approx -\delta_0 (\lambda^\pm)^2 / 2\pi b = -\delta_0 (1 \pm \sin \alpha)^2 / 2\pi p_\pm^2, \quad ,$$

so that the shift to the red of the peaks of the bands and the band widths are proportional to the square of the wavelength as for the case treated previously and as is required for self-consistency.

Substituting $\delta^\pm = \delta_0(1 \pm \sin \alpha)$ into T of (4.36) and its analogue for X^- yields

$$(4.36') \quad 2T = \sum \sigma^{-1/2} \left\{ \exp \left[i\sigma \delta_0 (1 \pm \sin \alpha) \right] + \exp \left[i\sigma \delta_0 (1 \mp \sin \alpha) + i\sigma 2p_\pm (1 \mp \sin \alpha) / (1 \pm \sin \alpha) \right] \right\} .$$

This reduces to $2T = \sum \sigma^{-1/2} \left\{ \exp \left[i\sigma \delta_0 (1 + \sin \alpha) \right] + \exp \left[i\sigma \delta_0 (1 - \sin \alpha) \right] \right\}$ for $\lambda^+ = \lambda^-$, when

$(1 \mp \sin \alpha) / (1 \pm \sin \alpha) = p_\mp / p_\pm$, which although not as simple as (4.30) (except for $\alpha = 0$) is of the same order of magnitude and indicates essentially the same sort of effects.

4.312 Numerical Analysis of the Solution

In this section the techniques and results of numerical investigation of the total scattered wave of (4.26) will be presented. This work was undertaken to support the physical arguments employed in the previous section for the derivation of the various general relations, and to check the validity of the assumption that δ_\wedge depended primarily on N and ϕ and only slightly on λ . The specific (and not necessarily realistic) numerical examples considered show that these arguments and this assumption were justified, and also substantiate the various figures of merit and relations for the ratio of the band widths, their structure, resolution, etc., that were obtained.

Employing the formalism of (4.30) for all values of λ for $A=2p_1\pi$ we write

$$(4.38) \quad T = \sum \sigma^{-1/2} e^{i\sigma\delta} = \mathcal{C} + i\mathcal{J}, \quad \delta = Kb(1 \pm \sin \alpha) - 2p_\pm \pi = Kb - 2p_\pm \pi,$$

where \mathcal{C} and \mathcal{J} are real. Employing the "Euler sum formula"¹⁰ to derive a more rapidly convergent representation for \mathcal{C} and \mathcal{J} yields

$$(4.39) \quad \mathcal{C} = \left(\frac{2\pi}{\delta}\right)^{1/2} \left[C(N\delta) - C(\delta) \right] + \frac{1}{2} \left(\frac{\cos N\delta}{N^{1/2}} + \cos \delta \right) - \frac{1}{12} \left(\frac{\delta \sin N\delta}{N^{1/2}} + \frac{\cos N\delta}{2N^{3/2}} - \delta \sin \delta - \frac{\cos \delta}{2} \right) \dots, \\ \mathcal{J} = \left(\frac{2\pi}{\delta}\right)^{1/2} \left[S(N\delta) - S(\delta) \right] + \frac{1}{2} \left(\frac{\sin N\delta}{N^{1/2}} + \sin \delta \right) + \frac{1}{12} \left(\frac{\delta \cos N\delta}{N^{1/2}} - \frac{\sin N\delta}{2N^{3/2}} - \delta \cos \delta + \frac{\sin \delta}{2} \right) \dots,$$

10. See for example L. Bieberbach, Lehrbuch der Funktionentheorie, Vol. I, p.307, Chelsea, New York, 1945.

where $C(N\delta)$, $S(N\delta)$, etc., are the tabulated Fresnel integrals¹¹. These are rapidly convergent for N large or δ small. Thus for $\delta = 0$, $\sum \sigma^{-1/2} = C \approx 2N^{1/2} - 1.46 + 1/2N^{1/2}$, yields results agreeing to at least three places for $N > 50$ with those obtained by adding the tabulated values of $\sigma^{-1/2}$. For $\delta \approx \pi$ retaining merely the terms indicated in (4.39) incurs an error of only about 5% for large N .

The function T , although the sum analogue of the integral yielding the Cornu spiral, yields a more complicated graph in the complex plane*. A plot of C vs. S for $\delta = 0$ to π resembles the sketch in Fig. 4.6 for large N , the "pigtail spiral" being more or less asymptotic to the 45° line with increasing N , but the

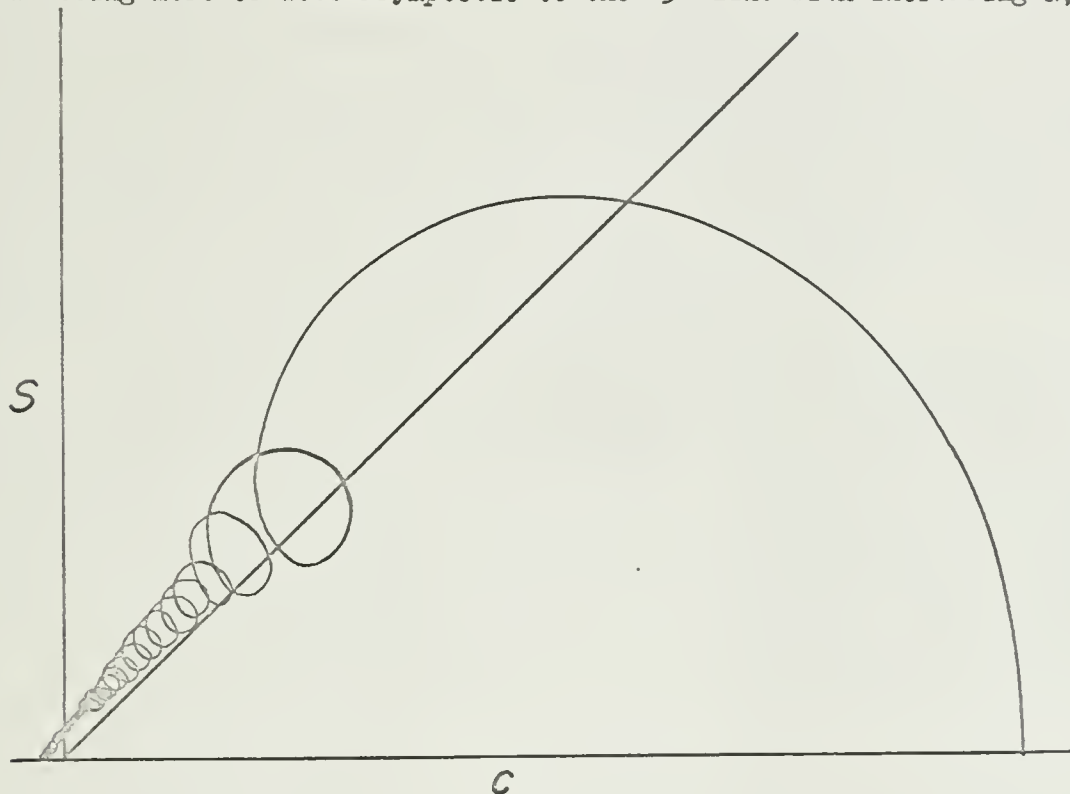


Fig. 4.6

curves for different values of N cannot be made to coincide by simply changing the scale factors. (For $\delta = 0$ to $-\pi$ we obtain the image of this curve in the real axis.) The periodicity of this spiral does not differ greatly from that of the Cornu spiral, as expected from (4.39), and the present curve is what would be "obtained" were we to shift the starting point of the Cornu spiral in the first quadrant to $\sum \sigma^{-1/2}$ along the real axis, and then pull its center out along the 45° line to about -0.5 . It can be seen that the previous considerations are on the whole valid, Fig. 4.3b,c

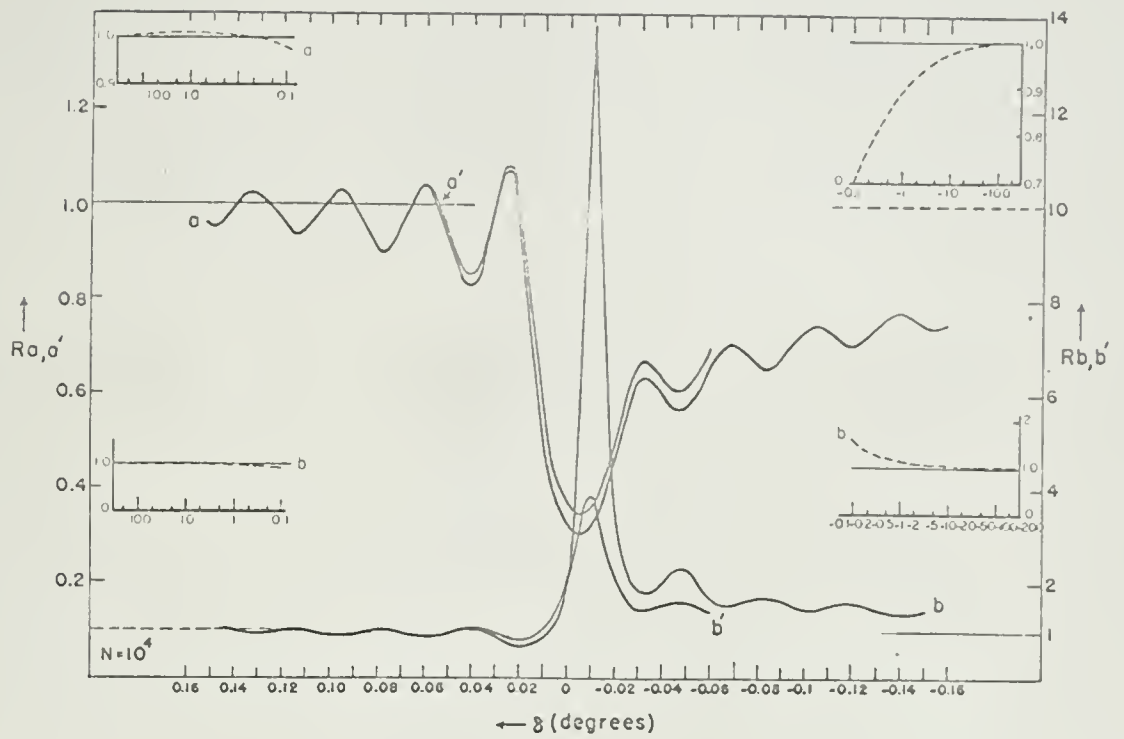
11. E. Jahnke and F. Emde, Tables of Functions, p.35, Dover, N.Y., 1945.

* This function has been analyzed graphically and numerically with N and δ as parameters; tables and curves will appear shortly in a report by Joy Bruno and the writer. Miss Bruno was also of great assistance in the numerical computations required for the graphs of the present paper.

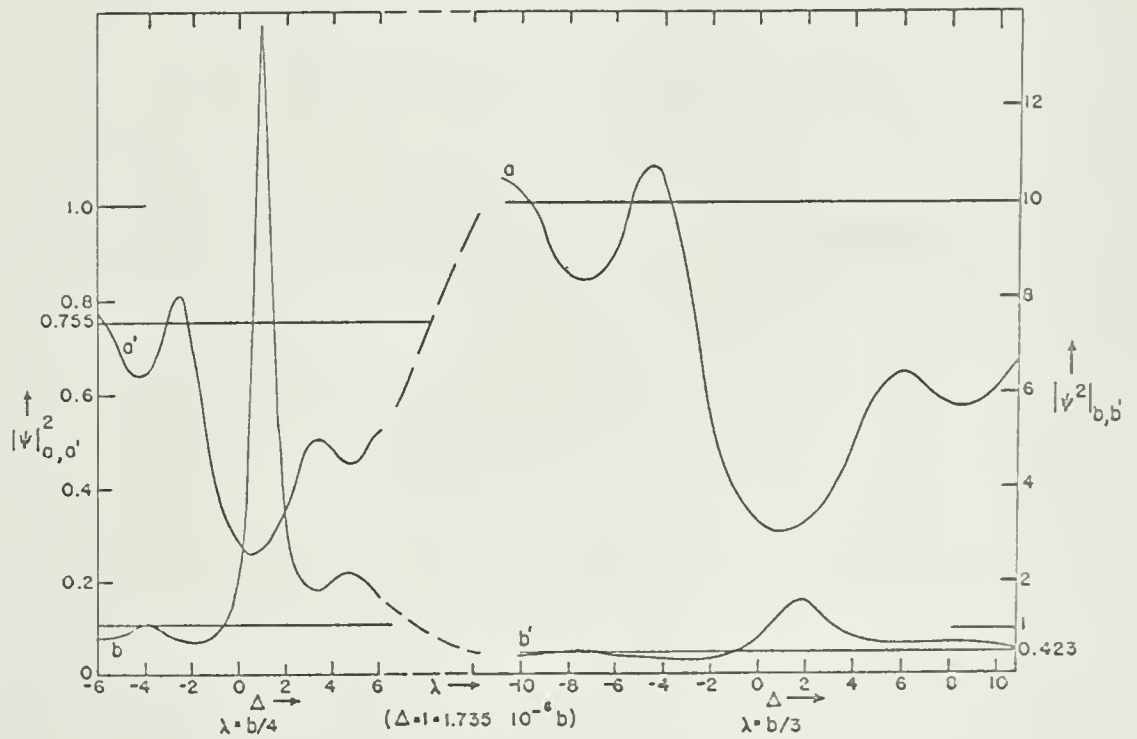
and d corresponding respectively to the first three intersections of the image of this curve with the -45° line, and Fig. 4.5 to portions of the curve parallel to the $+45^\circ$ line. The first intersection occurs for $|\delta| \approx 2.9\pi/4N$ for $N = 10^2, 10^3$ and 10^4 , which agrees with our previous upper limit $|\delta| \leq 3\pi/4N$.

Graphs 1, 3 and 4 are plots of $R = |\psi/\psi^1|^2$ vs. $\delta = Kb - 2p\pi$ in degrees for $N = 10^4, 10^3$ and 10^2 respectively. The a-curves, the dark bands, are for the perfect conductor, $\phi = \pi$ for $p = 3$, and the a'-curves or their remnants are for $p = 4$; the left R scale is to be used for these curves. The b-curves, or bright bands, are for the perfect dielectric, $\phi = 0$, for $p = 4$, and the b'-curves or their remnants are for $p = 3$; the right R scale, with a scalar factor one-tenth that of the left, is to be used for these curves. Note the reversal of the wavelengths, $\lambda = b/3, b/4$, for the primed and unprimed curves for $\phi = 0$ and π . The unprimed curves, corresponding to the wavelengths yielding the larger effects for the particular case, are associated with the longer wavelength for the perfect conductor and with the shorter wavelength for the perfect dielectric.

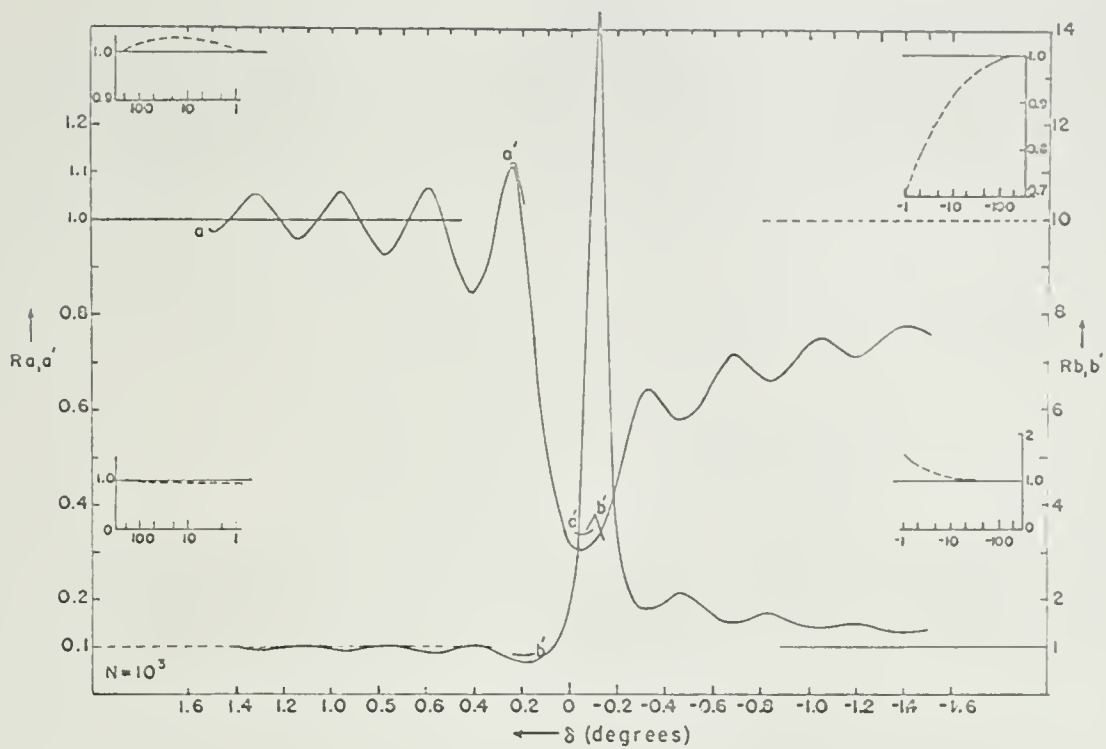
To facilitate comparison of the structure of these bands for different values of N , the same "normalization", $B_{\max} = B_0 2 \sum \sigma^{-1/2} / \pi p^{1/2} = 0.9$ ($\sum \sigma^{-1/2} = 198.5, 61.7$ and 18.6 for $N = 10^4, 10^3$ and 10^2 respectively), was chosen for the unprimed curves so that all the a-curves and all the b-curves have the same values of R for $\delta = 0$ for all N . This normalization prescribes different values for the ratio of the radius to spacing, say u , for each value of N and B_0 , u increasing markedly with decreasing N , particularly for the perfect conductor. Thus for curves a and a' we have $u = 2.53 \times 10^{-57}, 3.77 \times 10^{-19}, 3.93 \times 10^{-7}$, while for curves b and b', $u' = 5.37 \times 10^{-3}, 9.62 \times 10^{-3}, 1.75 \times 10^{-2}$, for $N = 10^4, 10^3, 10^2$, respectively. Hence the larger the value of u , the smaller the value of N required to obtain intensity ratios of the same order of magnitude. Although the present values of u , prescribed by the requirement that the series representation of (4.16) converges, do not seem particularly realistic for actual gratings, they indicate that the radius of the element should be quite small compared to spacing and wavelength for large N . We might also surmise that effects would in general be much less for relatively large radii $\approx \lambda$ because of the physical impossibility of satisfying the appropriate phase requirements over the entire surface of the elements. The normalization also prescribes the maximum value of B for the primed curves so that for the a'-curves $B_{\max} = 0.782, 0.784, 0.798$, for $N = 10^4, 10^3, 10^2$, while for the b'-curves $B_{\max} = 0.585$ for all N .



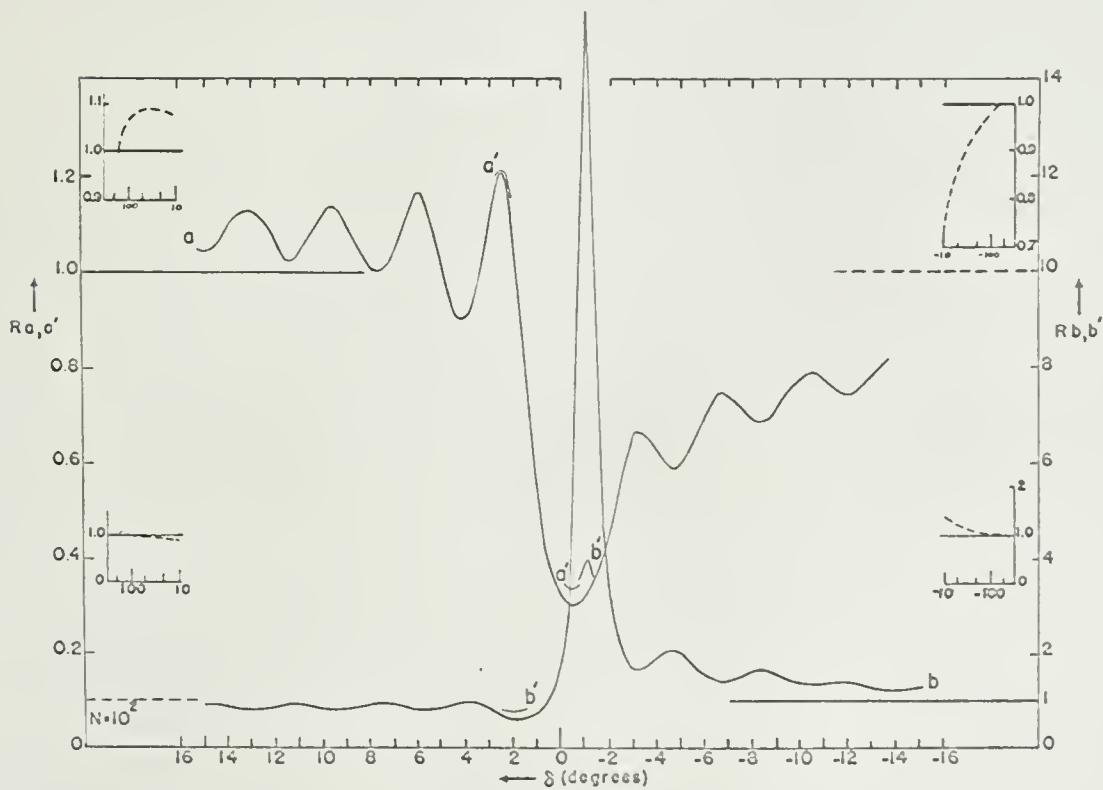
Graph 1



Graph 2



Graph 3



Graph 4

Our previous surmise that the value of δ corresponding to the maximal effects depended primarily on N for a given value of λ_0 is substantiated by these curves, there being only a very slight shift to a smaller value of δ for the larger λ_0 . Although corresponding curves of the graphs cannot be made to coincide by superposition, the deviations are relatively superficial and the positions of the local extrema agree closely on a scale of δ/N . Thus the peaks of the maximal bright bands occur for $\delta \approx -2.4\pi/4N$, while the "peaks" of the dark bands fall at $\delta \approx -1.1\pi/4N$. It can be seen that the largest absolute slopes occur for the short wavelength side of the peaks as deduced previously.

Our previous considerations as to the character and positions of the local extrema are valid in their essentials. Although the departures of R from unity are more pronounced on the long wavelength side of λ_0 , than those of their complements for $\lambda < \lambda_0$, the former approach unity more rapidly than the latter as $\delta \rightarrow \pi$. Taking into consideration the logarithmic scales of the inserts (showing mean values of R for $|\delta|$ approaching the minimal value of 180°) we surmise that a more detailed investigation will show that energy is conserved in the process. The distance between the local extrema flanking the peak is approximately $550^\circ/N$, or differs by less than a factor of 2 from the value $8\pi/4N$ employed previously as a figure of merit. The peak of the bright band, however, is narrower than that of the dark, and is also more pronounced because of its relatively less prominent local extrema.

The "contrast" of the bands, or R_{\max}/R_{\min} , increases with increasing λ_0 for the perfect conductor and decreases with increasing λ_0 for the perfect dielectric, the change being much more pronounced for the second of these. The contrast also increases, and the peak effects become more marked, with decreasing N for the same normalization. We note that the total scattered intensity ranges from about 0.3 to 15.5 times its single scattered value for the various curves.

We could interpret these curves for R as corresponding physically to values obtained for fixed angles of incidence and observation with incident monochromatic radiation of different wavelengths, for which case the graph of $|\psi^1|^2$ would be that of the principal maximum and secondary maxima of $\Delta(n)$ corresponding to these angles. We choose, however, to regard these graphs, and those of $|\psi^1|^2$ to be discussed shortly, as corresponding to values obtained for a fixed angle of incidence but with varying monochromatic radiation and with varying angle of observation, the angle of observation being that which yields a principal maximum for the particular wavelength under consideration. Hence the single scattered intensity, equalling $|\psi^1|^2 = \eta_{B_0}^2/2\pi\epsilon r$, can be considered as constant in the immediate vicinity of λ_0 and identical for curves a and b by virtue of the normalization.

Were we to ignore possible discrepancies arising from the neglected end effects, the shortcomings of the mode hypothesis, and the presence of the transmitted

plane wave, and were we to assume in addition that the spectral lines of $\Delta(\lambda)$ were of infinitesimal width, we could regard these curves as corresponding to spectrograms in the vicinity of the λ_0 's for incident white light. Because of the finite width of a principal maximum of $\Delta(\lambda)$ and because of its secondary maxima, however, there will always be present some "background" light of different wavelength than that corresponding to a particular angle of observation; i.e., for a single scattering or Fraunhofer grating and incident white light, intensity measurements for a particular angle of observation should give lower readings if a narrow pass filter corresponding to the narrow range of wavelengths supposedly falling on the instrument is placed between the instrument and the grating. To facilitate further discussion and comparison with experiment, however, we accept these curves as corresponding to spectrograms for white light, but expect that many of their finer details will not be detected experimentally.

Graph 2 which is a plot of $|\psi|^2$ vs. λ for the parameters of graph 1 (unity on the intensity scale equalling $|\psi^1|^2$ with $\lambda = b/3$, $\phi = \pi$ or $\lambda = b/4$, $\phi = 0$) is therefore regarded as approximating an experimental intensity curve in the vicinity of the λ_0 's. We expect, however, that rather than our oscillatory bands, "wedges" bounded sharply on their short wavelength side and "tailing off" on the long wavelength side will be observed experimentally. The widths of the peaks are $1.025 \times 10^{-5}b$ for $p = 4$ and $1.82 \times 10^{-5}b$ for $p = 3$ so that their ratio is 9/16 as determined previously; the bands with their tails are of course much wider than these values, but the ratio should be preserved. The darker band occurs for the shorter wavelength for the perfect conductor and for the longer wavelength for the perfect dielectric.

The quantity $|\psi|^2$ can be considered as proportional to the total intensity or Poynting flux provided that $\Delta(\lambda)$ is sufficiently large so that the effects of the incident wave and the cross terms due to interference of the incident and scattered waves can be neglected. For the minima of $|\psi|^2$, however, or in general when λ is small these must be taken into account as in (1.35, 48) to obtain the total physical fields and derived quantities for comparison with experiment. To evaluate these quantities we require

$$(4.40) \quad \rho = \operatorname{Re}(w e^{-iKrcos(\theta+\alpha)}) = DR(\cos q - B \cos q'),$$

where $D = \Delta(\lambda) B_0 (2/\pi Kr)^{1/2}$, $R = 1/(1 - B e^{i\beta})|^2$, $q = Kr[1 - \cos(\theta + \alpha)] + \phi + \pi/4$, and $q' = q - \beta = Kr[1 - \cos(\theta + \alpha)] - \gamma$. For D very large these terms are in general negligible compared to $|\psi|^2 = D^2 R$, particularly for R large. For moderate values of D and R small, however, they may need to be taken into account. Thus when successive orders are out of phase we have $\rho = -D \cos \left\{ Kr[1 - \cos(\theta + \alpha)] + \pi/4 \right\} / (1 + B)$ and $|\psi|^2 = D^2 / (1 + B)^2$. The largest values of B are of the order of unity so that the first term is proportional to $D/2$ as compared to $D^2/4$ for the second. If these two terms are of the

same order of magnitude, or if the first is much greater than the second, the intensity curves will be quite different from those we've considered. More generally the plane wave and interference terms will tend to smooth out the local extrema to form a gradual tail for the effects.

We note that the convergence requirement, $B_{\max}^2 < 1$, for a given value of N , λ , and b/r furnish an upper limit for the single scattered intensity, or D^2 , provided we assume that $\mathcal{N} = 2N+1$ or that N is essentially the total number of pairs of cylinders (rather than some fraction). Thus since $|\psi^1|^2 = D^2 = B_{\max}^2 (N/t_m)(b/r) \leq (N/t_m)^2 (b/r)$, and since we require that $Nb \ll r$, we have $D^2 < N/t_m^2$. Using our previous values for $t_m = \sum \sigma^{-1/2}$ we have $t_m^2 \approx 4N$. Hence we obtain $D^2 < 1/4$ so that the plane wave and the interference term need to be taken into account, particularly for the minima. It can be seen that the convergence requirement necessitates that the usual Fraunhofer effects be weak for these gratings if N is of the order of $\mathcal{N}/2$.

4.32 " A_1 mode"

For a plane wave polarized perpendicular to the axis of a dielectric cylinder, or for a gaseous cylinder in acoustics, and $Ka \rightarrow 0$, the largest coefficient is $A_1 = iB_1 e^{i\phi}$ as in 1.62, 65, 66. Retaining only this coefficient, and provided that $|A_1 X|^2 < 1$, we obtain from (4.20)

$$(4.41) \quad \psi = \sum \psi^m = \Delta(\mathcal{N}) H_0 2A_1 \left[\cos\theta \cos\alpha - \sin\theta \sin\alpha / (1 - 2A_1 X) \right] \\ = \psi_e^1 + \psi_o^1 / (1 - 2A_1 X) = \psi_e + \psi_o .$$

To our present order of approximation only the odd component, or that symmetrical with respect to the plane of the grating is effected by multiple scattering, the solution reducing to that predicted by single scattering theory for normal incidence or observation. With increasing α and θ the odd component becomes more effective (plots of R for $\psi_e \approx \psi_o$ would differ greatly from those discussed previously), until finally for either grazing incidence or observation the total scattered wave is formally identical with ψ of (4.23) for the dielectric case.

Hence for large α and θ for a perfect dielectric maximal effects of the same type occur for both the perpendicular and parallel components and at the same wavelengths. However since the present $2B$ equals $2/(k_0+1)$ times the B that occurred for the parallel component, and also because of the "background" factor $\cos\theta \cos\alpha$, the effects are less pronounced for the present case. For the conducting dielectric the phase factors ϕ are no longer zero and maximal effects occur at different wavelengths for the perpendicular and parallel components.

The total scattered intensity and the interference term are given by

$$|\psi|^2 = 4D^2 \left\{ \cos^2 \theta - R_0 \sin \theta \sin \alpha - 2B \cos \beta \cos \theta \cos \alpha - \sin \theta \sin \alpha \right\} ,$$

$$\rho = 2D \left\{ \cos \theta \cos \alpha - R_0 \sin \theta \sin \alpha - 2B \cos \beta \right\} ,$$

where $R_0 = |1/(1-2Be^{i\beta})|$ and where the remaining symbols are as for (4.40) but with B_0 , β replaced by B_1 , β_1 as in (1.62, 65, 66).

4.33 "A₀ + A₁ mode"

For a plane wave polarized perpendicular to the axis of a perfectly conducting (or ferromagnetic) cylinder, or for a rigid cylinder or one of large impedance in acoustics and $Ka \rightarrow 0$,

$$A_0 = iB_0 e^{i\beta_0} \text{ and } A_1 = iB_1 e^{i\beta_1} .$$

Retaining only these coefficients, we can rewrite (4.40), which we rewrite, by combining

all the terms symmetrical in α and θ in the quotient, as

$$(4.43) \psi = \Delta(\mathcal{N})H_0 \left\{ \frac{A_0(1 - \cos \theta \cos \alpha)}{(1 - A_0 X)} + \frac{X + 2A_0 A_1 (\sin \alpha - \sin \theta) Y}{-2A_0 A_1 Y^2} + 2A_1 \cos \theta \cos \alpha \right\} ,$$

where Y is obtained from $X \propto T_- + T_+$ by changing the sign of T_+ . If $A_0 = -A_1$, (4.43)

reduces to

$$(4.43') \psi = \Delta(\mathcal{N})H_0 A_0 \left\{ \frac{1 + 2A_0 X + 2 \sin \theta \sin \alpha (1 - A_0)}{(1 - A_0 X)(1 + 2A_0 X)} - \frac{(\sin \alpha - \sin \theta) Y}{2Y^2} - 2 \cos \theta \cos \alpha \right\} .$$

For $Kb \sin \alpha = 2p'\pi$, Y vanishes and (4.43) reduces

$$(4.44) \psi = \psi_0^1 / (1 - B^0 e^{i\beta_0}) + \psi_{10}^1 / (1 - 2B^1 e^{i\beta_1}) + \psi_{1e}^1 = \psi_e ,$$

where ψ_0^1 is the first order scattered wave containing only A_0 and similarly ψ_1^1 contains only A_1 , the subscripts o and e indicate odd and even, and where $B^j = B_j 2t(2/\pi Kb)^{1/2}$ and $\beta_j = \beta_j + \gamma + \pi/4$ with $j = 0, 1$.

For perfectly conducting (or rigid) cylinder, $B^j = -A_1 = -i\pi X^2/4 = iB_0 e^{i\pi}$,

and (4.44) reduces to

$$(4.44') \psi = \psi_0^1 / (1 + B e^{i\beta}) + \psi_{10}^1 / (1 - 2B e^{i\beta}) + \psi_{1e}^1 ,$$

where $B = t x^2 (\pi/2Kb)^{1/2}$, $\beta = \gamma + \pi/4$ and $\psi^1 = \Delta(\mathcal{N})H_0 A_0 [1 - 2 \cos \theta \cos \alpha]$. Thus for normal incidence or observation, or α or θ small, the maxima and minima give rise to intensity minima or dark bands, essentially as for the parallel polarization component for perfectly conducting cylinders, although these must now contend with the background factor $-2 \cos \theta \cos \alpha$. For $\alpha = 0$, $\theta = \pi/2$, or vice versa, (4.44) is formally identical with (4.23). For a given grating and λ , however, the effect is much less for this case than for the previous logarithmic coefficient, while the contrasts and intensities of the bands vary with wavelength as they did for the previous case of the perfect dielectric. Thus $B \propto \lambda^{-3/2}$ increases rapidly with decreasing λ , so that the most pronounced departures from single scattering theory occur for the shorter wavelengths, although these are not necessarily the darkest bands since the intensity ($\propto \lambda^{-3}$) increase as λ decreases. (See the 0-curves in graphs 5 and 10 in the section on the

reflection grating, which correspond respectively to $\lambda = b/4$, $b/3$, for the case of $\alpha = 0$, $\theta = \pi/2$. Although the contrast is greater for the first, or shorter wavelength, the darkest bands occur for the longer wavelength, unity on graph 10 equaling 0.422 of that on graph 5. The remaining plots are graphs of $|\psi|^2$ with ψ as in (4.44') but without the cosine term.)

For α and θ large, and θ positive, ψ_0 predominates and the maximal effects give rise to intensity maxima or bright bands (as for the perfect dielectric for the isotropic case) so that the effects are of opposite type to those that occurred for the parallel component and perfectly conducting cylinders. For α and θ large, and θ negative, the intensity for certain values of δ may approach zero, the even term cancelling the remaining terms, to yield much more pronounced dark bands than for the parallel component. For arbitrary α and θ , the odd and even components of ψ compete to determine the character of the band, and its structure can only be determined by numerical calculations. Thus for $\sin \alpha = 1/4$ the band at $\sin \theta = 0$, $q = +1$, is dark while those at $\sin \theta = 1/4, 1/2, 3/4, 1$, $q = +2, +3, +4, +5$ are bright bands, the intensities increasing with increasing θ ; while for $\sin \theta = -1/4, -1/2, -3/4, -1$, $q = 0, -1, -2, -3$ the bands are initially dark bands but develop into "double bands" of a peculiar structure having both a pronounced maximum and minimum. (These observations are based on graphs 7 and 8 of the section on the reflection grating.)

Rewriting (4.44') as

$$(4.44'') \psi = -D i^{1/2} \exp(iKr) \left\{ 1 - 2\cos(\theta + \alpha) - B e^{i\beta} \left[\frac{1}{(1 + B e^{i\beta})} - 4\sin\alpha \sin\theta / (1 - 2B e^{i\beta}) \right] \right\},$$

we see that for the forward scattered wave or central maximum, $\theta = -\alpha$, the curly bracket yields $\left\{ -1 - B e^{i\beta} \left[\frac{1}{(1 + B e^{i\beta})} + 4\sin^2\alpha / (1 - 2B e^{i\beta}) \right] \right\}$ so that for the vicinity of the maximal effects, $\beta \approx 0$, the intensity $|\psi|^2$ is greater than its single scattered value for all values of α . For the back scattered wave, however, $\theta = \pi - \alpha$, and the curly bracket reduces to $\left\{ 3 - B e^{i\beta} \left[\frac{1}{(1 + B e^{i\beta})} - 4\sin^2\alpha / (1 - 2B e^{i\beta}) \right] \right\}$ so that the intensity in the vicinity of the maximal effects is less than its single scattered value for α small and greater for α large. The structure of these bands is in general much more complicated than for the A_0 mode, the band width and other features depending on both angular parameters. (See graphs 5, 6, etc. for the analogous situation for the reflection grating.)

The total scattered intensity and the interference term are given by

$$(4.45) |\psi|^2 = D^2 \left\{ 4\cos^2\alpha \cos^2\theta + 4R_1 \sin^2\theta \sin^2\alpha + R_0 + 4R_1 r \sin\theta \sin\alpha - 4\cos\theta \cos\alpha \left[R_0 (1 + B \cos\beta) + 2\sin\theta \sin\alpha R_1 (1 - 2B \cos\beta) \right] \right\},$$

$$\rho = -D \left\{ -2\cos\theta \cos\alpha \cos q + R_0 (\cos q + B \cos q') + 2\sin\theta \sin\alpha R_1 (\cos q - 2B \cos q') \right\},$$

where $R_0 = (1+2B\cos\beta+B^2)^{-1}$, $R_1 = (1-4B\cos\beta+4B^2)^{-1}$, $r = (1-B\cos\beta-2B^2)$ and where the remaining parameters are as for (4.40) with $\phi = 0$, $B_0 = \pi\chi^2/4$. We will consider the analogous expressions for the reflection grating, which are somewhat simple, in greater detail in the following section.

We note that the jargon of this theory which was developed initially for the case where essentially only one scattering coefficient of the single cylinder was considered, is on the whole fully applicable to the present case provided that we retain the notion of a "mode hypothesis", i.e., the maximal effects for each mode occur for the wavelengths which insure optimal fulfillment of the conditions that each order of scattering of the mode is a maximum and that successive orders of scattering of the mode are either in or out of phase. For the problem of the perfect conductor, the maximal wavelengths (as well as those for the local extrema) are essentially the same for each mode (although the effects for each mode are of opposite character), so that the resultant peak effects should occur in their immediate vicinity and somewhat close to those of the dominant mode. This is certainly plausible for the bright peaks but it is conceivable that the minima of the dark bands may be shifted appreciably for θ and α on opposite sides of the surface normal, for which case the darkest parts of the bands may be determined by annulment between the modes rather than by the phase relations of the orders of scattering. Because of "mode competition" the shapes of the bands may also differ appreciably from those of a single mode, and the width of the peaks and the strengths of the local extrema become functions of the angular parameters. More generally, when the phase factors of the two scattering coefficient do not differ by π and when the modes have the same sign, the effects of mode competition should be less pronounced but the displacement of the resultant maximal wavelengths greater. It is also evident from the form of ψ of (4.18) that we need never be concerned with more than two modes or components for $A = 2p'\pi$, i.e., an even component and an odd component which are the resultants of all the even and odd coefficients of the single cylinder respectively.

4.4 The Reflection Grating of Bosses on a Plane

Consider a plane wave incident on a reflection grating of parallel semi-cylindrical bosses of arbitrary physical parameters on a perfectly conducting (or rigid) infinite plane as at the right in Fig. 4.7. Applying the image technique discussed in section 2, we treat the problem of two plane waves, which are images in the removed plane, simultaneously incident on the grating of parallel cylinders; the "image problem". The technique of solution is indicated schematically in the figure.

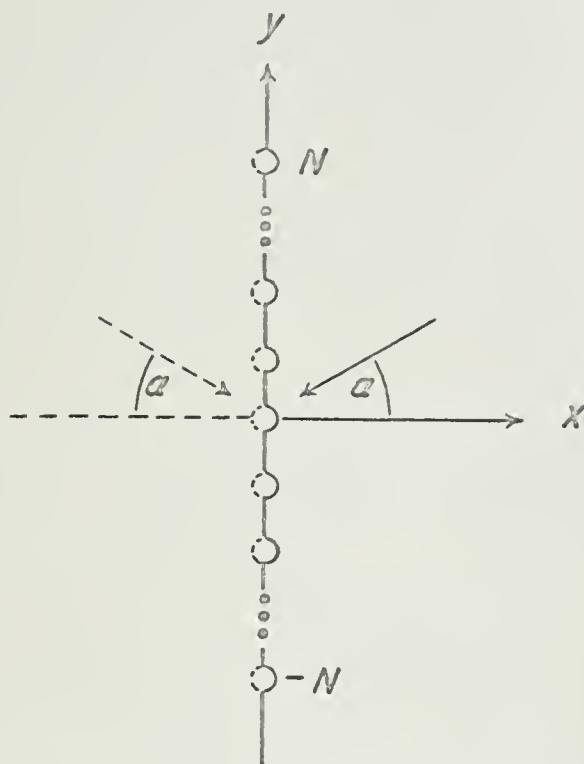


Fig. 4.7

For the component polarized perpendicular to the cylinders' axis or parallel to the plane of incidence (or for the acoustic case of a rigid plane), the total incident wave for the image problem is $\psi_i = \psi_1(\theta) + \psi_1(\pi - \theta) = \exp[iKrcos(\theta + \alpha)] + \exp[-iKrcos(\theta - \alpha)]$, the second of these indicating that the previous θ is to be replaced by $(\pi - \theta)$. The total scattered wave is then $\psi'' = \psi(\theta) + \psi(\pi - \theta)$, where $\psi(\theta)$ is as in (4.3, 19, etc.), and the total reflected wave for the boss problem is $\psi_r'' = \psi_1(\theta) + \psi''$; we have chosen to regard $\psi_1(\pi - \theta)$, the wave on the right in Fig. 4.7 as the incident wave for the boss problem, and $\psi_1(\theta)$ as the specularly reflected component. Thus we obtain

$$(4.46) \quad \psi'' = 2H_0 \Delta(\eta) [C_+ + Q],$$

where $C_+ = \sum \epsilon_n A_n \cos n(\alpha + \pi/2) \cos n(\theta - \pi/2)$, and where Q is the quotient of (4.19, 19').

For the component polarized parallel to the cylinders' axes or perpendicular to the plane of incidence (or for the acoustic case of a plane of zero impedance), the total incident wave is $\psi_i(\theta) - \psi_1(\pi - \theta)$, the total scattered wave is $\psi' = \psi(\theta) - \psi(\pi - \theta)$, and the total reflected wave $\psi_r' = \psi_1(\theta) + \psi'$. Thus from

(4.19) we obtain

$$(4.47) \psi' = 2H_0 \Delta(\eta) C_-, \quad C_- = -2 \sum_n A_n \sin n(\alpha + \pi/2) \sin n(\theta - \pi/2),$$

or the value obtained previously subject to the single scattering approximation^{2,12}, the multiply scattered contributions vanishing because of their symmetry with respect to the plane of the grating for $Kb \gg 1$.

For this order of magnitude these expressions indicate that the effects of multiple scattering should appear primarily for the component polarized perpendicular to the axes of the elements (which is in agreement with the observations of Wood⁴, Strong⁵ and Ingersoll⁶). Thus if the bosses are dielectric and $x' \ll 1$ (the A_1 mode), we obtain

$$(4.48) \psi'' = 2\psi_0, \psi_0 \text{ as in (4.41); } \psi' = 0.$$

The function ψ'' is also the scattered wave for the acoustic case of gaseous bosses on a rigid plane. If the first two coefficients of the single cylinder are retained (the $A_0 + A_1$ mode), we obtain

$$(4.49) \psi'' = 2\psi_0, \psi' = 4A_1' H_0 \Delta(\eta) \cos \theta \cos \alpha,$$

where ψ_0 is the function of (4.43, 44) without the $\cos \theta \cos \alpha$ term. The function ψ'' is the scattered wave for the perpendicular polarization component for perfectly conducting bosses or bosses of arbitrary impedance on a rigid plane, while ψ' corresponds to the parallel polarization component for perfectly conducting bosses or bosses of arbitrary impedance on a surface of zero impedance. For the perfect conductor we have simply $A_0 = A_1' = -i\pi x^2/4$ so that for $A = 2p'\pi$ we obtain

$$(4.49') \psi'' = -D \exp \left[i(Kr + \pi/4) \right] \left\{ 1/(1 + Be^{i\beta}) + 2 \sin \theta \sin \alpha / (1 - 2Be^{i\beta}) \right\},$$

$$\psi' = -2D \exp \left[i(Kr + \pi/4) \right] \cos \theta \cos \alpha$$

where $D = \Delta(\eta) x^2 (\pi/2Kr)^{1/2}$, $B = tx^2 (\pi/2Kb)^{1/2}$, $\beta = \gamma + \pi/4$, and $T = te^{i\gamma} = \sum \sigma^{-1/2} e^{i\sigma Kb}$,

We see therefore that the scattered component polarized perpendicular to the axes of the bosses will exhibit the same sort of bright and dark bands for particular values of Kb as appeared previously for both polarization components for the grating of cylinders. We will shortly discuss ψ'' of (4.49') in detail; for the moment we will consider ψ' , which should also show these anomalies even if to a lower order of magnitude.

Proceeding to the next order of magnitude in Kb for the parallel component we obtain from (4.7) that

$$(4.50) \psi' = 4A_1' H_0(r) \Delta(\eta) \cos \theta \cos \alpha / \left[1 - A_1' X(H_0 + H_2) \right],$$

where $A_1^i = A_0 = -i\pi x^2/4$, and $X(H_0 + H_2) = \sum [H_0(\sigma Kb) + H_2(\sigma Kb)] \cos(\sigma Kb \sin \alpha)$. However, since $H_0 + H_2 = 2H_1/\sigma Kb \approx -i2H_0/\sigma Kb$, we see that the maximal effects are much smaller for this case than for the perpendicular component. Thus we have

$$(4.50') \quad \psi^i = \psi^i / [1 + (i2A_0/Kb)X^i] = -2D \exp[i(Kr + \pi/4)] \cos \theta \cos \alpha / [1 + (2/Kb)B^i e^{i\beta^i}],$$

where $X^i = 2 \sum \sigma^{-1} H_0(\sigma) \cos A$, $B^i = t^i x^2 (\pi/2Kb)^{1/2}$, $\beta^i = \gamma^i - \pi/4$ and

$$t^i e^{i\gamma^i} = T^i = \sum \sigma^{-3/2} e^{i\sigma Kb} \cos(\sigma Kb \sin \alpha). \quad \text{The effects of multiple scattering}$$

should therefore also be observed for the parallel polarization component for the reflection grating, particularly for the longest wavelengths of the order of magnitude of the spacing, but the departures from single scattering theory should be much less pronounced than for the perpendicular component.

To obtain some idea of the relative magnitudes for the effects for the two components we note that $\sum \sigma^{-3/2} \approx 2.3, 2.5$ for $N = 10^2, 10^4$ respectively as compared with $\sum \sigma^{-1/2} \approx 18.6, 199$ for those two values of N . Assuming that $Kb \approx 10$, β and $\beta^i \approx 0$, and $B \approx 0.8$ so that $R = (1+B)^{-2} \approx 0.31$, yields $R^i = (1+2B^i/Kb)^{-2} \approx 0.96, 0.996$ for $N = 10^2, 10^4$ respectively and the effects are negligible for the parallel component. We note, however, that for other values of the parameters R^i may differ appreciably from unity, and also that for certain values of α and θ the parallel effects may be more pronounced than the perpendicular, the maximal effects yielding a dark band for the former, and a dark or bright band for the latter as determined by α and θ . The most interesting feature of these "parallel anomalies" for the reflection grating is that since $\beta^i = \gamma^i - \pi/4$, γ^i and consequently δ_\wedge , as in (4.30), must be positive quantities, hence the darkest part of the band is on the short wavelength side of $\lambda_0 = b/p$, or the peak effects are shifted to the blue rather than the red side of λ_0 .

Faint parallel anomalies were observed by Wood⁴ with reflection gratings yielding pronounced perpendicular anomalies but these were not investigated. More recently a detailed investigation of these anomalies was carried out by Palmer¹³, one of Strong's students, but the results have not yet been made available. It should be noted that Rayleigh's dynamical theory of grating⁷ does not predict the presence of these parallel anomalies.

We will now consider the total scattered intensity for the perpendicular component as in (4.49'), or for a rigid surface in acoustics, in detail. We have

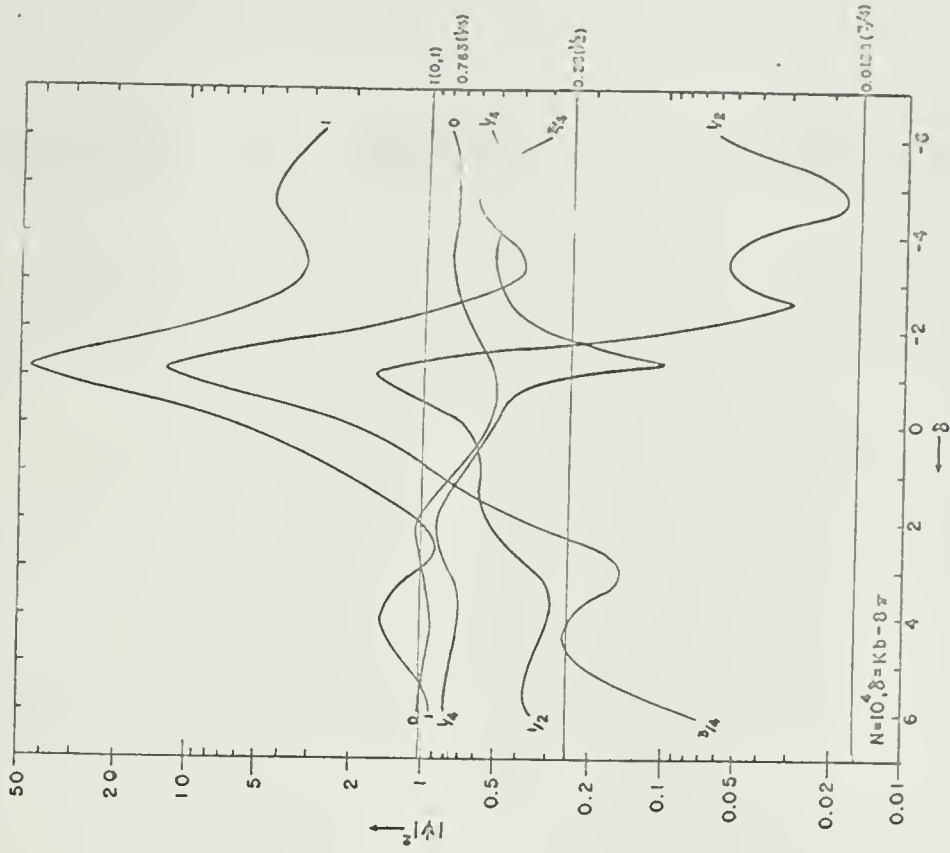
13. C.H. Palmer, Doctoral Dissertation, Johns Hopkins University, 1951.

$$(4.51) \quad |\psi''|^2 = D^2(R_0 + 4R_1 \sin^2 \theta \sin^2 \alpha + 4R_0 R_1 r \sin \theta \sin \alpha),$$

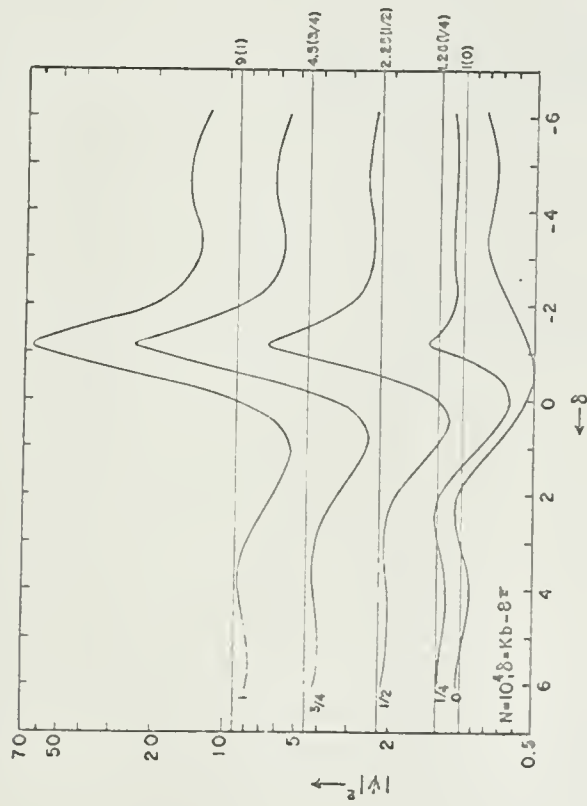
where R_0 , R_e and r were defined for (4.45), and their parameters for (4.49'). The essential features of this expression were discussed with reference to (4.41') for the transmission grating (which had an additional term in $\cos \theta \cos \alpha$); it differs significantly from that obtained for isotropic scatterers in that the character of the bands depend markedly on α and θ .

Graphs 5 - 9 are plots of $|\psi|^2$ vs. $\delta = Kb - 2p\pi$ for $N = 10^4$, for $\lambda = b/4$ and graphs 10 - 14 are the corresponding plots for $\lambda = b/3$. It is assumed in these curves, as in the previous, that θ is varied with λ to correspond to a principal maximum of $\Delta(\eta)$ for a given value of α so that $|\psi^1|^2$ can be considered constant for each curve, the simple trigonometric function, $(1 + 2\sin \alpha \sin \theta)^2$, being insensitive to the small variations of θ this requires for δ small. The "normalization" for all the curves is $2B_{\max} = 0.9$ for $\lambda = b/4$ so that the ratio of boss radius to spacing is $a/b = 3.8 \times 10^{-3}$, while the maximum value of $2B$ for $\lambda = b/3$ is 0.585. Unity on the logarithmic intensity scales for $\lambda = b/4$ is D^2 while that for $\lambda = b/3$ is 0.422 times this quantity; the single scattered values are indicated on the right scale.. It should also be kept in mind that since $\Delta_3 = 16 \Delta_4/9$, the bands for $\lambda = b/3$ are about 1.78 times the width of those for $\lambda = b/4$ on a wavelength axis.

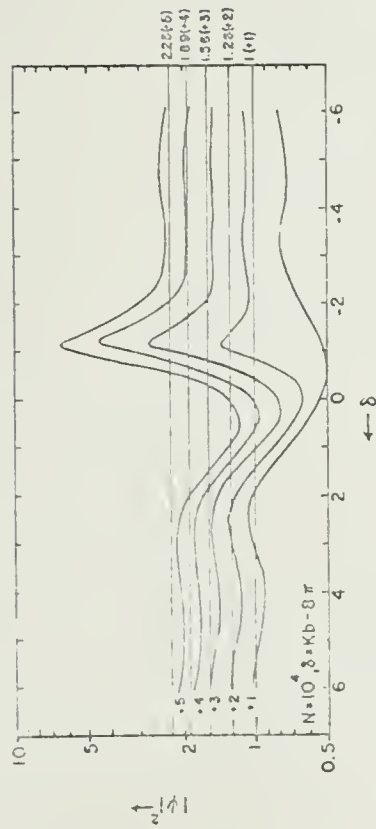
Graphs 5 and 10 which are plots for the back scattered intensity in the vicinity of $\theta = \alpha = \sin^{-1}(p'/p)$, $p' = 0, 1, \dots, p$, indicate that the bands which are dark for normal incidence grow into bright bands with increasing α and θ , the maximum shifting to the long wavelength side of the minimum. The greatest departures from single scattering theory, $R_{\Lambda} = R_{\max}$, $R_{\vee}^{-1} = R_{\min}^{-1}$ ($R = |\psi/\psi^1|^2$), and the contrasts, R_{Λ}/R_{\vee} , increase in general with increasing α (curves marked 1/4 and 1/3 are exceptions) and are greater for the shorter wavelength. The darkest bands, however, occur for the longer wavelength. Graphs 6 and 11 which are plots of the "forward scattered" intensity, or central maximum, in the vicinity of $\theta = -\alpha = -\sin^{-1}(p'/p)$, $p' = 0, 1, \dots, p$, indicate that with increasing α the bands initially become more pronounced dark bands but that as α increases further they turn into bright bands, the maximum (which has broadened a great deal) shifting to the long wavelength side of the minimum. We note that in this process bands may appear which have a pronounced maximum but "tail off", or have their most pronounced local maxima on their short wavelength side as in the 2/3-curve, while other bands may be "double" possessing both a marked maximum and minimum as in the 1/2-curve. The maximal departures and the contrast initially increase with increasing α but fall off as α increases still further. These are in general greater for the shorter wavelength. The 3/4-curve, one of the exceptions to this as far as R^{-1} is concerned, is in this region of δ entirely above its single scattered value but this



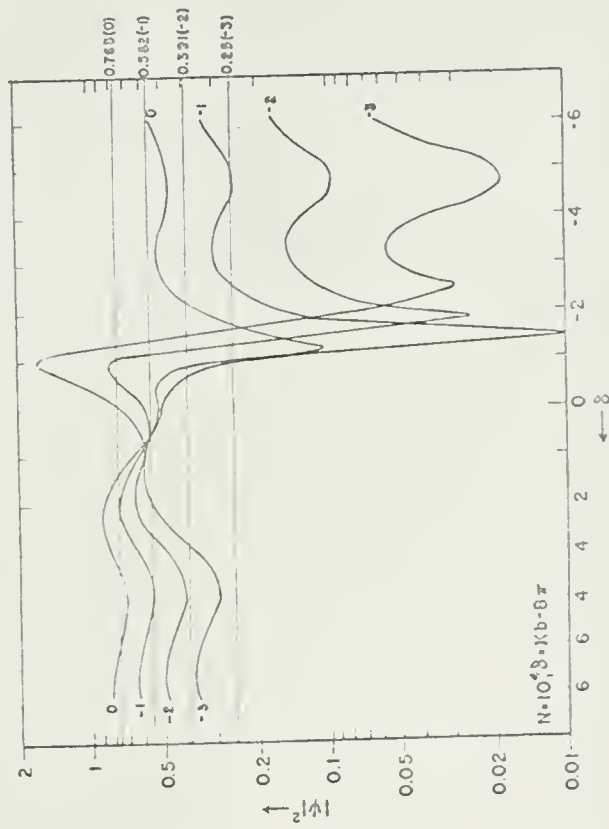
Graph 5



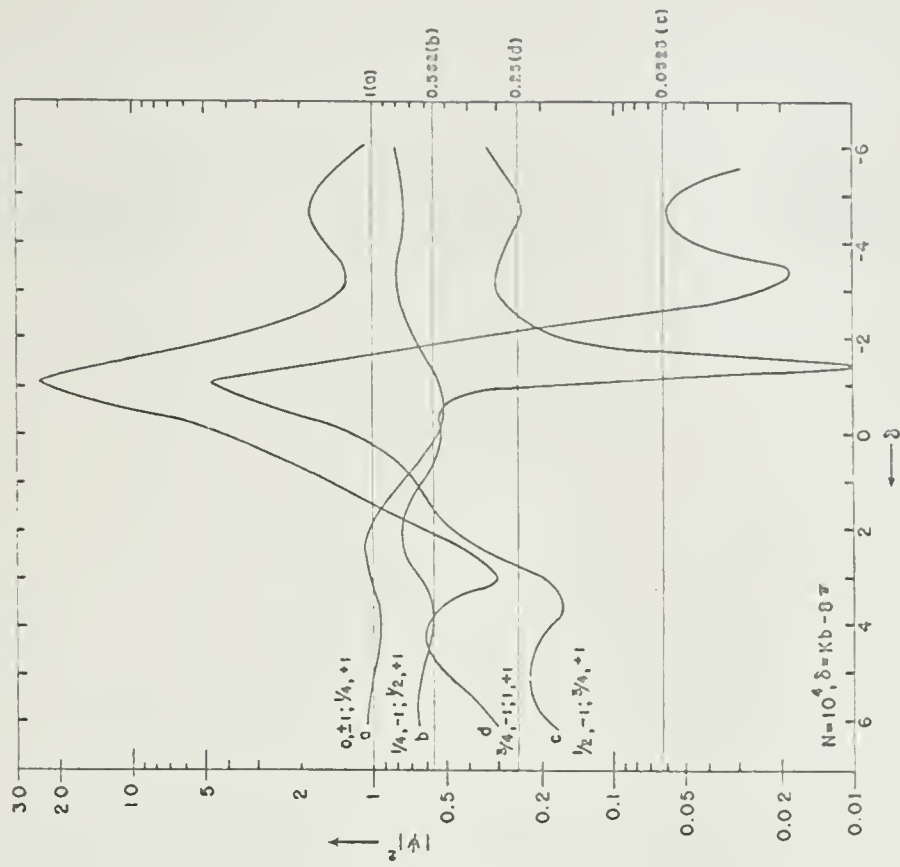
Graph 6

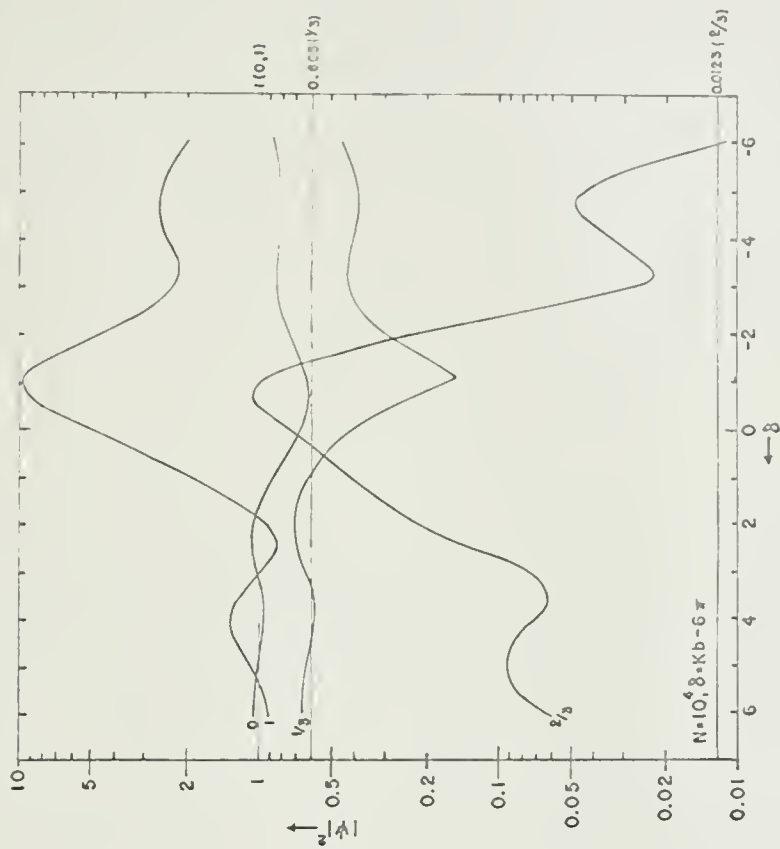


Graph 7

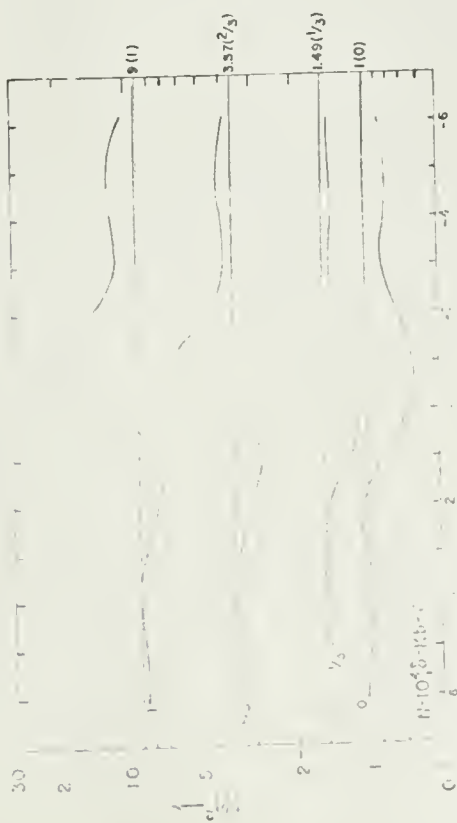


Graph 8

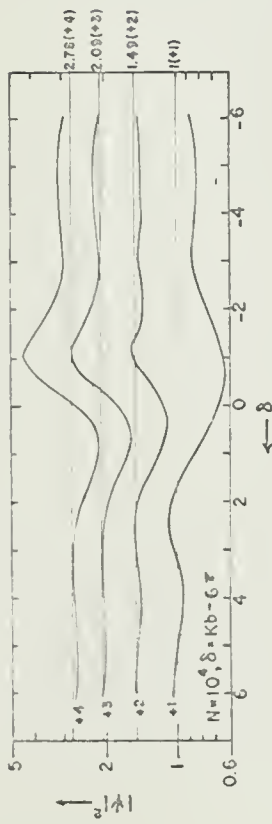




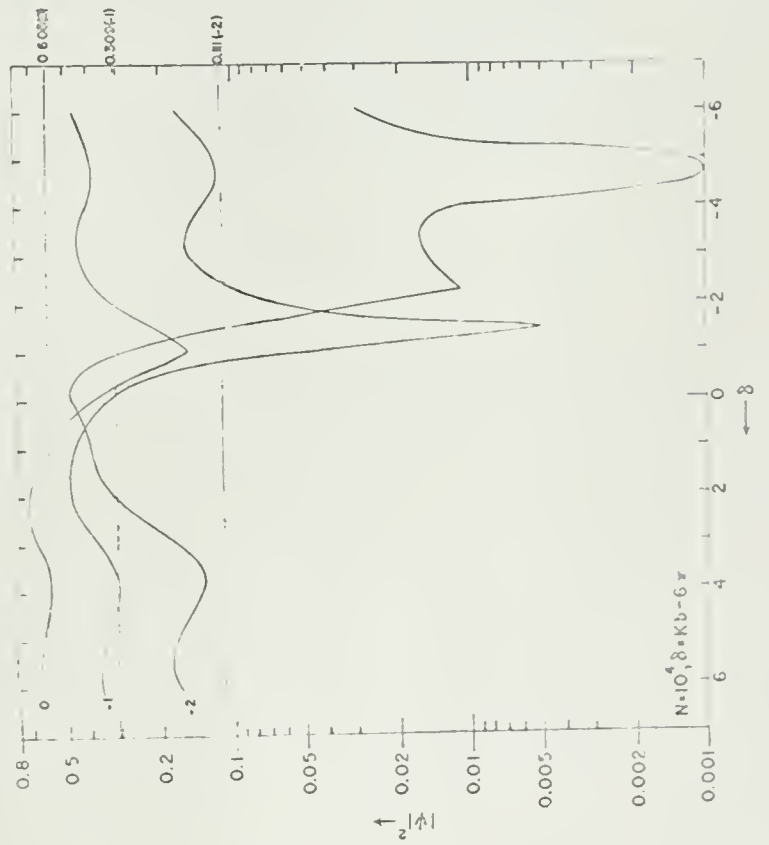
Graph 11



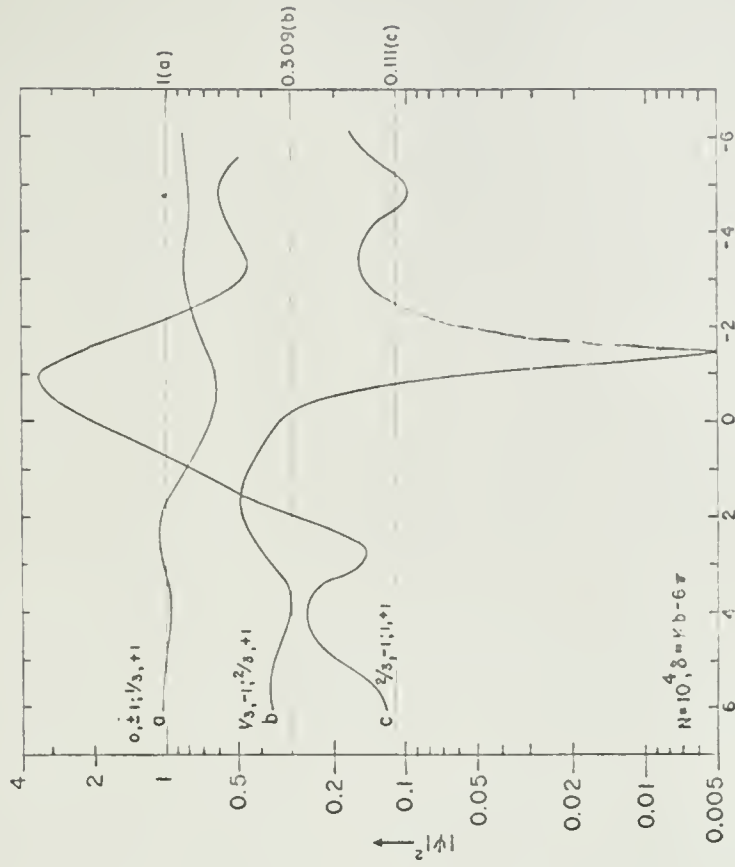
Graph 10



Graph 12



Graph 13



Graph 14

increase of energy is no doubt compensated for by corresponding decreases for larger values of δ , or in some other order. The value of $R_{\Lambda} \approx 800$ for the $3/4$ -curve, or the total scattered intensity of the order of 800 times its single scattered value, is the largest intensification we have encountered.

Graphs 7 and 12 are plots of the scattered intensity for the positive orders for $\sin \alpha = 1/p$ and graphs 8 and 13 show the central maximum and negative orders; the positive orders lie on the side of the central maximum towards the source, or counter clockwise from the direction of the image wave (the direction of the central maximum) in Fig. 4.7. The behavior of the curves for the positive orders with increasing q is essentially as for the back scattered waves of graphs 5 and 10 with increasing α (although the growth is more gradual and the effects not so pronounced), while the curves for the central maximum and the negative orders are all dark bands whose complexity increases with increasing q , one of the local minima finally turning into the darkest part of the band. It can be seen that R_{Λ} for the negative orders is in general greater for the shorter wavelength, while R_{Λ}^{-1} and $R_{\Lambda}/R_{\Lambda'}$ are greater for the longer wavelength, i.e., the more pronounced intensification occurs for $\lambda = b/4$ while the more pronounced reduction (as well as the darker bands) and bands of greater contrast occur for $\lambda = b/3$ for the negative orders. The value of $R_{\Lambda} \approx 0.009$ for $\lambda = b/3$, $q = -2$, or the total scattered intensity less than one-hundredth of its single scattered value is the largest reduction we have encountered; note that unlike the case of isotropic scatterers $|\psi|^2$ may equal zero when the curly bracket of (4.49') vanishes for certain values of the parameters with α and θ on opposite sides of the surface normal, i.e., for the value $\sin \theta \sin \alpha = -(1-2B)/2(1+B)$, provided that θ and α are permissible values. The value of $R_{\Lambda}/R_{\Lambda'} \approx 480$ for this curve is the greatest contrast yet encountered and this band is also the darkest.

Graphs 9 and 14 are plots of the scattered intensity for $\sin \alpha = p'/p$, $p' = 0, 1, \dots, p$, and $q = \pm 1$; each set corresponds to two sets of values because of the reciprocity of θ and α . Increasing α from 0 to $\pi/2$ and observing the positive order we go through curves a, a, b, c, (d), while for the negative order we go through a, b, c, (d). Both sets of orders start out initially as dark bands and end up as bright but the effects for $q = +1$ "lag" those for $q = -1$, the same curves appearing for $q = +1$ for a larger value of α . Comparison of graph 9 with 6 and 14 with 11 indicates that for a given value of α the bands for the central maximum and one of the adjacent orders may "tail off" in a direction opposite to the band of the remaining adjacent order, while for other values the bands for the central maximum and one adjacent order may complement the character of the band of the remaining order. Thus $\sin \alpha = 1/2$, $q = 0$ and -1 show maxima while

$q = +1$ is a pronounced minimum; $\sin \alpha = 3/4$, $q = 0$ and -1 yield pronounced bright bands completely above their single scattered values for this region of δ , while for $q = +1$ the maximum tails off in the opposite direction; $\sin \alpha = 2/3$, $q = 0$ and -1 show marked maxima tailing off in opposite directions while $q = +1$ is a pronounced minimum; and finally for $\sin \alpha = 1$, $q = 0$ and $+1$ show the same sort of bright bands for both sets. (This sort of behavior has been observed by Wood⁴ and Strong⁶.) The intensification, R_{\wedge} , increases with α for both wavelengths, the effect for the shorter being greater; the reduction, R_{\vee}^{-1} , has its greatest values for the b-curves where the effect is greater for the longer wavelength, although for the other curves the effects are greater for the shorter; while the contrast has its greatest value for the c-curve for the longer wavelength and for the b-curve for the shorter, the values being greater for the longer except for curve b. We note that for $q = +1$ the bands for $\sin \alpha = 0$, $1/4$ are identical while the minimum for $\sin \alpha = 1/2$ is much narrower; similarly for $q = +1$, $\sin \alpha = 0$, $1/3$ and $\sin \alpha = 2/3$. (This sort of behavior seems to be indicated by Fig. 1.3, Wood⁴ (1935) which corresponds to our Fig. 4.4 with reversed λ - axis.)

It should be noted that for many cases the width of the maximal peak is either much greater or much less than that obtained for isotropic scatterers. It should also be noted that several of the curves appear on more than one graph and also that the accuracy of the computations for the curves, which is in general of the order of 5% , decreases rapidly as $|\psi|^2 \rightarrow 0$.

These curves were computed for $N = 10^4$, but as can be seen from comparison of graphs 1, 3 and 4, we would obtain essentially the same results for $N = 10^3$ and 10^2 . Since $\delta_{\wedge} \propto N^{-1}$, however, the numerical values on the δ -scale would be multiplied by 10 and 100, and similarly for the spread on the λ -scale, for $N = 10^3$ and 10^2 respectively.

For simplicity we have considered only the contribution scattered by the grating in the above. More generally, however, we must consider the total reflected wave, or the sum of the scattered component and the specularly reflected image wave. Thus for an incident wave as in Fig. 4.7, the mirror image of \underline{E}^1 of (1.37) or

$$(4.52) \quad \underline{E}^p = \left\{ -A [\sin(\theta-\alpha)\hat{r} + \cos(\theta-\alpha)\hat{\theta}] + B\hat{k} \right\} \exp[-iKrcos(\theta-\alpha)] ,$$

$$\underline{E}^p = \gamma \left\{ B [\sin(\theta-\alpha)\hat{r} + \cos(\theta-\alpha)\hat{\theta}] + A\hat{k} \right\} \exp[-iKrcos(\theta-\alpha)] ,$$

where A and B are the amplitudes of the incident components polarized perpendicular and parallel to the axes of the bosses, the total reflected fields and intensities are as in (1.48). The required interference terms are

$$(4.53) \rho'' = -D[R_0(\cos q + B \cos q') + 2R_1 \sin \theta \sin \alpha (\cos q - 2B \cos q')],$$

$$\rho' = -2D \cos \theta \cos \alpha \cos q$$

where the notation is as for (4.51). The discrepancies that may arise between the curves here presented and those obtained experimentally, and their causes, are essentially as for the transmission grating and isotropic scatterers as discussed previously with reference to graphs 1 - 4. See also discussion of (4.40) for the effects of the plane wave component.

4.5 Extension of the Theory to Gratings with Elements other than Cylinders.

In this paper we have presented a multiple scattering theory of the grating of cylinders. A formal solution to the mathematical problem was obtained, approximate solutions were analyzed in detail, and the results were compared with experiment. The departures from elementary theory that the present theory predicts were correlated with the experimental "grating anomalies," and their presence interpreted plausibly on the basis of simple physical arguments.

Only gratings of circular cylinders or semicylindrical bosses on a plane were considered, but it is evident from the structure of the analysis that the theory can be extended to transmission gratings whose elements are elliptical cylinders, as well as to the corresponding reflection gratings. For the restrictions for which the solution in closed form obtains, (4.19), the appropriate representations for certain cases can be written down by inspection; similarly, for the limiting cases of very small elements, analogous mode approximations, in which only one or two scattering coefficients of the single element are retained, can be found.

The significance of the scattering coefficient of the single element in controlling the form of the intensity curves is evident from the preceding sections. Although the physical condition that each order of scattering of the grating by a maximum is independent of the elements, being identically (4.12) for all gratings, fulfillment of the conditions that successive orders be in or out of phase is dependent on the phase of the scattering coefficient (or the material and polarization component). Similarly the contrast and the overall intensity of the bands as a function of λ depends on the form of the amplitude of the coefficient. Thus for the cases treated in graphs 1 - 4, the bands were dark or bright as the phase was 0 or π , while the contrast and overall intensity increased with λ for the logarithmic coefficient and decreased for the coefficient in λ^{-2} . Similarly for two modes, where the additional factor of mode competition exists, the bands were bright or dark depending on the dominant mode as determined by the angular parameters and the phases of the coefficients, while the contrast and overall intensity were in general larger for the shorter wavelength because of the λ^{-2} behavior of both coefficients.

We can extend our theory to gratings with elements other than cylinders by employing the approximate solutions for a perfectly conducting single strip and a single slit in a perfectly conducting plane which were derived by Rayleigh¹⁴. For the strip and perpendicular polarization, or for the slit and parallel polarization, he obtained essentially that $A_0 = 0$, $A_1 = A_1^0$, or the A_1 mode with A_1 as for a perpendicular polarization for a perfectly conducting cylinder whose diameter equalled the slit or strip width. Similarly for the strip and parallel polarization, or the slit and perpendicular polarization, he obtained $A_0 = A_0^0$, or the A_0 mode with A_0 as for parallel polarization for a perfectly conducting cylinder. The extension of multiple scattering theory to these elements can be carried out by substituting these values into the expressions we've derived, a grating of narrow strips corresponding to our transmission grating of cylinders, and that of slits to our reflection grating.

It is tempting to extend Rabinet's principle, as illustrated by the above to the analogous pair of the semicylindrical boss and a semicylindrical depression; the second of these is a very difficult problem mathematically and little has been accomplished towards its solution. Proceeding formally, we replace the coefficient amplitudes in λ^{-2} for the perpendicular polarization component by the logarithmic amplitude that appeared for the parallel component, and vice versa, to obtain expressions indicating essentially the same sort of bands occurring for the same wavelengths and angles as for the bosses, and differing only in that their contrasts and relative intensities increase with increasing λ rather than decrease as for the bosses. Could such a procedure be justified, we would obtain a more suitable model for the reflection grating with grooves narrow compared to wavelength. We have brought this point up to indicate the basis of the only marked discrepancy between our theoretical results for the reflection grating of bosses and the available experimental results for narrow-grooved gratings; the experimental results show the same increase of contrast with increasing λ that is deduced from the expressions obtained by extending Rabinet's principle to the boss to obtain the solution for the depression.

The experiments of Wood⁴, Strong⁵, Ingersoll⁶, and Palmer¹³ mentioned previously were performed with essentially two types of reflection gratings. In some cases the anomalies could be traced to the presence of fine ridges or protuberances bordering the usual grating grooves (as was deduced on the disappearance of the anomalies from the spectra by gently rubbing the grating), while in others it was surmised that the effects were due to the very narrow grooves themselves. Our results are in good agreement with these experiments, particularly

14. Rayleigh, Phil. Mag. 43, 259 (1897)

with those for the "ridged" gratings for which Wood⁴ (1935) also observed fainter anomalies polarized parallel to the elements. The intensity curves we have sketched are in general more complicated than those obtained experimentally, but the reasons for this are probably due to the assumptions we have made to obtain approximate solutions, to the presence of the incident and reflected plane waves as discussed previously, and to the effects of the particular groove form; the last of these is perhaps the most significant factor. The asymmetry of the usual grating groove results in the multiple excitations traveling in one direction along the grating differing in amplitude and phase from those traveling in the other direction, and accounts for the absence or disappearance of certain of the branches in Wood's spectrograms (reference 4, 1935, Fig. 1.3), and also for the fact that in many cases the intensity of these branches differ little from the intensity at the "intersections", i.e., where $A = 2p'\pi$. (Note that for these cases, where only the waves going up or down the grating exists, the solution is of the form of (4.18").) Similarly exact correspondence is not expected for the ridged gratings since they actually comprise two superposed gratings, one of fine ridges which multiply scatters, and one of the wide grooves which only singly scatters; for the second of these, presumably the large width of the grooves compared to wavelength precludes satisfying the optimal phase relations required for pronounced multiple scattering effects. Such gratings therefore possess additional background Fraunhofer spectra which mask some of the effects of the ridges.

.....

The next paper of this series will treat multiple scattered reflection from a striated surface consisting of parallel bosses on a plane.

APPENDIX

Derivation of (4.19')

Wilhelm Magnus

We will derive $Z = \sum_{m=2}^{\infty} f^m$, where $f^m = \psi^m / H_0 \Delta(\mathcal{H})$, with ψ^m as in (4.16').

From an examination of the multiple sum it follows that it can be written as a power series in S_- , S_+ with coefficients which are of the type

$$(1) \quad \begin{array}{ll} C^i (C^0)^k (\underline{C}^0)^{\ell} C^{\prime\prime} & C^i (C^0)^k (\underline{C}^0)^{\ell} \underline{C}^{\prime\prime} \\ \underline{C}^i (C^0)^k (\underline{C}^0)^{\ell} C^{\prime\prime} & \underline{C}^i (C^0)^k (\underline{C}^0)^{\ell} \underline{C}^{\prime\prime} \end{array}$$

We shall write Z in the form

$$(2) \quad Z = C^i C^{\prime\prime} K_{11} + C^i \underline{C}^{\prime\prime} K_{12} + \underline{C}^i C^{\prime\prime} K_{21} + \underline{C}^i \underline{C}^{\prime\prime} K_{22} ,$$

where the $K_{\nu,\mu}$ ($\nu, \mu = 1, 2$) are power series in S_- , S_+ with coefficients which are multiples of products of powers of C^0 , \underline{C}^0 .

From the general expression for Z we find that the first terms of K_{11} are

$$(3) \quad K_{11} = S_- + S_-^2 C^0 + S_-^3 (C^0)^2 + S_-^2 S_+ \underline{C}^0 C^0 + \dots$$

The terms of K_{11} arise from the following process:

We consider a product of $(\ell+1)$ brackets -

$$(4) \quad \left[S_- + (-1)^{n+n'} S_+ \right] \left[S_- + (-1)^{n'+n''} S_+ \right] \dots \left[S_- + (-1)^{n^{(\ell)}+n^{(\ell+1)}} S_+ \right] .$$

Any term arising from the multiplication of these brackets which is involved in K_{11} must necessarily be such that the first and the last bracket contribute the factor S_- . This follows from the assumption that K_{11} involves the terms to which the C_n^i , $C_n^{\prime\prime}$ contribute a factor which is a product of $C^i C^{\prime\prime}$. Now let us denote by D_{ℓ} the terms of K_{11} which are of degree $\ell+1$ in S_- , S_+ . Let us split D_{ℓ} into a sum

$$(5) \quad D_{\ell} = u_{\ell} + v_{\ell} ,$$

where u_{ℓ} involves all the terms of D_{ℓ} which are obtained by choosing S_- as the contribution of the ℓ^{th} (the second but last) factor in (4). Similarly, let v_{ℓ} denote the terms which arise if we take

$$(6) \quad (-1)^{n^{(\ell-1)}+n^{(\ell)}} S_+$$

as the contribution of the ℓ -th bracket. Then we claim that:

$$(7) \quad \begin{aligned} u_{\ell+1} &= u_{\ell} S_- C^0 + v_{\ell} S_- C^0 \\ v_{\ell+1} &= u_{\ell} S_+ \frac{(C^0)^2}{C^0} + v_{\ell} S_+ C^0 \end{aligned}$$

Indeed, if we take a product of $(\ell+2)$ bracket, in (4) and put the last one aside (since in our case, S_- has to be taken as the contribution of this factor), we see that the term S_- in the $(\ell+1)$ -th factor contributes both $u_\ell S_- C^0$ and $v_\ell S_- C^0$ to $u_{\ell+1}$. The factor

$$(8) \quad (-1)^{n^{(\ell)}+n^{(\ell+1)}} S_+$$

necessarily will contribute to $v_{\ell+1}$. If combined with the terms represented by u_ℓ , it will influence both the summation of the $C_n^0(\ell)$ and of the $C_n^0(\ell+1)$. Since the summation of the $C_n^0(\ell)$ in u_ℓ contributed a factor C^0 , and since now both summations contribute a factor \underline{C}^0 , the total contribution of (8) to $v_{\ell+1}$ is,

$$u_\ell S_- \frac{(\underline{C}^0)^2}{C^0}.$$

On the other hand, the influence of (8) on v_ℓ is simply an exchange of a factor C^0 in the ℓ -th place and a factor \underline{C}^0 in the $(\ell+1)$ th place. That accounts for the term

$$v_\ell S_- C^0$$

in (7).

This shows that $u_{\ell+1}$, $v_{\ell+1}$ are connected with u_ℓ , v_ℓ by a linear substitution, the matrix

$$(9) \quad M = \begin{pmatrix} S_- C^0 & S_- C^0 \\ S_+ \frac{(\underline{C}^0)^2}{C^0} & S_+ C^0 \end{pmatrix}$$

of which does not depend on ℓ . Since

$$I + M + M^2 + M^3 + \dots = (I - M)^{-1},$$

where I denotes the identity:

$$I = \begin{pmatrix} 1 & 0 \\ 0 & 1 \end{pmatrix},$$

and since

$$u_1 = S_-^2 C^0, \quad v_1 = 0,$$

we find after an elementary calculation

$$(10) \quad K_{11} = D_0 + \sum_{\ell=1}^{\infty} (u_\ell + v_\ell) \frac{1 - S_+ C^0}{1 - (S_- + S_+) C^0 + S_- S_+ [(C^0)^2 - (\underline{C}^0)^2]}.$$

The coefficients K_{12} , K_{21} , K_{22} can be computed by the same method. The denominator, which is the determinant of $I - M$, will always be the same.

FEB 28 1954

DATE DUE

MAY 19 1961

144-1.1.93

GAYLORD

PRINTED IN U.S.A.

NYU
EM-
39 Twersky

c.1

Multiple scattering of
radiation, Part II

NYU
EM-
39 Twersky

c.1

AUTHOR

Multiple scattering of

TITLE

radiation, Part II

DATE
DUE

BORROWER'S NAME

ROOM
NUMBER

MAY 1 1981 ~~STICKLER~~

1-1-93 ILL - NAVAL COMMAND

N.Y.U. Courant Institute of
Mathematical Sciences
4 Washington Place
New York 3, N. Y.

